Wave-speed limitation on expiratory flow-a unifying concept

S. V. Dawson and E. A. Elliott

J Appl Physiol 43:498-515, 1977. ;

Wave-speed limitation on expiratory flow—a unifying concept

STANLEY V. DAWSON AND EDWARD A. ELLIOTT
Department of Physiology, Harvard School of Public Health, Boston, Massachusetts 02115

DAWSON, STANLEY V., AND EDWARD A. ELLIOTT. *Wave-speed limitation on expiratory flow—a unifying concept.* J. Appl. Physiol.: Respirat. Environ. Exercise Physiol. 43(3): 498–515, 1977.—The mechanism limiting forced expiratory flow is explained on the basis that a local flow velocity reaches the local speed of wave propagation at a point, called the choke point, in intrathoracic airways. This theoretical approach to the "waterfall effect" leads to selection of the analogy of constricted open-channel flow to apply to the elastic network of airway tubes. Quantitative results are derived for the case of negligible friction by use of the Bernoulli principle. Shapes predicted for the maximum-flow static recoil curves depend only upon the nature of the pressure-area curve at the choke point in the case of negligible friction; and the magnitude of the critical rate of flow depends on reference values of cross-sectional area and elastic modulus at the choke point, on gas density, and on the static recoil pressure. The present theoretical results are used to interpret previous experiments, but quantitative applicability is limited because of frictional effects and lack of knowledge of choke point conditions.

aerodynamics of lungs; choke point; collapsible tubes; elastic tubes; flow limitation; flow-volume curves; isovolume-pressure-flow curves; lung airways; maximum flow; waterfall effect

THE MAXIMUM EXPIRATORY FLOW-VOLUME (MEFV) curve is a display of the maximum expiratory flow rate over the whole range of vital capacity (VC) of the lung. Such curves are largely reproducible in any given subject because, beyond a critical level of effort, the flow is independent of pleural pressure, which is a measure of the effort furnished by the chest wall (4). This independence of effort, taken together with the observed dependence of maximum flow on lung volume, strongly suggests that there is within the lung a mechanism which limits the expiratory flow. The present work is a theoretical study of this mechanism and how it produces the observed MEFV curves.

The earliest mathematical approach to the explanation of expiratory flow limitation was that of Fry (7). His model was based on the differential equation of flow in a uniform elastic tube situated in a pressure environment like that of the pleural pressure of the lung. According to the predictions of this model, the flow as a function of pleural pressure would have a maximum and not a plateau. In later work Weibel's symmetrically branching model of lung airways was used with various assumptions about airway elasticity and friction laws in order to predict maximum flow (8, 20, 30). Neither that work nor a related analysis (2) offered an adequate explanation of the observed plateau of flow at pleural pressures above the critical value.

The mechanism of expiratory flow limitation has also been described intuitively on the basis of observation of lung airways during forced expiration. Experimental observations have shown that under conditions of flow limitation the airway approaching the thoracic outlet is highly compressed because the pleural pressure generated by effort of the chest wall greatly exceeds the hydrostatic pressure within the trachea. Pride et al. (33), referring to the earlier work of Permutt and coworkers on hemodynamics of collapsible vessels, called attention to the compressed airway. They postulated that the effect occurring there was like that of a waterfall, in which reductions of downstream water level below a certain critical level do not influence the flow. In the situation of lung airways, the increase of pleural pressure (effort) above the critical value translates into a decrease of transmural pressure below a critical value at the thoracic outlet. This value of transmural pressure is the analog of the level downstream of the waterfall. The analysis proceeded in terms of "resistances," defined as the ratio of pressure drop to flow rate, both upstream and downstream from an especially collapsible segment of airway. Mead et al. (27), on the other hand, in considering the condition of flow limitation at any particular lung volume, focused attention on the airway upstream from the equal pressure point (EPP), at which the pressure within the airway exactly equals pleural pressure. They noted that the pressure drop from alveolus to EPP is just the static recoil pressure of the lung. So this pressure drop is independent of effort, as is the flow at limitation. Therefore the ratio of this pressure drop to flow has a value which depends on lung volume but is independent of effort. They considered this ratio to be an "upstream resistance," which being independent of effort implies that the airway geometry upstream from the EPP is fixed for all pleural pressures higher than the critical value.

In work outside lung mechanics, it has been predicted that flow limitation in elastic tubes would occur at the speed at which the fluid in the tube propagates pressure waves. These waves, which arise from the interaction of radial recoil force of the elastic wall and the axial inertial force of the fluid, are the pulse waves of blood flow. The basic speed of propagation of these pressure waves is $(Y/\rho)^{1/2}$, where Y, as defined mathematically below, is the elastic modulus (reciprocal of specific compliance) of

the tube cross section (lumen) and ρ is the density of fluid within the tube. In the absence of longitudinal tension along a simple tube of circular cross section and for small motions from the condition of no distending pressure, this is the same wave speed as obtained by Young in 1808 (24, see also APPENDIX A and Table 1). In a review article on blood flow, R. T. Jones argued that the steady force balance, which he computed from the Bernoulli principle, would become unstable if attempts were made to force fluid through an elastic tube at velocities higher than the wave speed (18). The limitation of steady flow at wave speed was developed for key situations in simple elastic tubes by Griffiths in a theory of male micturition (11), which followed from his earlier theory that the maximum flow rate in the female urethra would have a velocity equal to wave speed at an elastic constriction. See also the analysis of Oates (28).

The wave-speed theory of flow limitation has been extensively studied in two fluid mechanical situations: the constricted open hydraulic channel, a situation including the waterfall, and the gas nozzle. Both situations have a common analysis in terms of velocity and also in terms of "pressure condition," which is taken to be the absolute pressure in the gas nozzle and the water level in the hydraulic open channel (see Fig. 1, *A* and *D*). It is this analysis that is extended in the present work to elastic tubes, especially lung airways (see Table 2, which summarizes the various terminologies).

In both the constricted hydraulic channel and the gas nozzle, we consider an upstream reservoir with sufficient inflow to keep its pressure condition fixed. The reduction of pressure condition in a downstream reservoir or other point for controlling pressure downstream from some constriction then causes flow to increase up to a critical rate such that the speed of wave propagation in the flow is reached at the constriction. In Fig. 1, *B* and *E*, curve 2 corresponds to a condition in which a decrease of downstream pressure causes an increase of flow. Notice the depression of pressure condition due to the increased velocity at the constriction. Curve 3 is the critical curve for which the velocity reaches wave speed at the constriction, which becomes a point where flow is choked or limited. Further decreases in downstream pressure, as in curve 4, do not alter the flow rate but merely determine the pattern downstream from the choke point. A physical explanation of the limitation is that disturbances cannot propagate upstream if the velocity of flow faster than the propagation speed; so the downstream changes in level cannot travel upstream through the choke point to affect flow rate. The region between the choke point and the downstream point of control in curve 4 adjusts itself so that the velocity is above wave speed upstream and below wave speed downstream from an energy-dissipating transition. For

TABLE 1. *Excised dog airways: minimum average wave speed*

	Y,† cmH_2O	$(Y/\rho)^{1/2}$, cm/s
Trachea	36	6×10^3
Medium bronchus	9	3×10^3
Small bronchus	1	1×10^3

† $Y \equiv A\partial B/\partial A$ scaled directly from the maximum compliance point of the Martin and Proctor data (24) as presented in Fry's (8) Fig. 4.

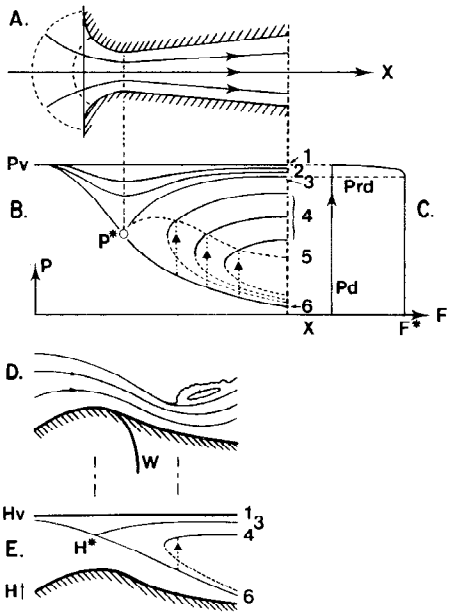

FIG. 1. Well-known examples of flow limitation. *A*: flow in a gas nozzle from an upstream reservoir. *Solid curves* represent streamlines with velocity in direction of arrows. Choke point occurs at smallest cross section (= throat), where velocity is sonic. *B*: pressure along length of nozzle for fixed upstream reservoir pressure Pv and various downstream pressures: *1*) Pd = Pv, no flow. *2*) Entirely subsonic flow. Note the depressed pressure, indicating increased velocity, at the constriction (nozzle throat). *3*) Curve for critical flow rate. Speed of sound is reached at the throat where P = P*. Remainder of curve is subsonic. Flow remains exactly at critical value for all lower downstream pressures. *4*) Downstream pressure below critical value. Jump in pressure (shock) is indicated by dotted line from P* −6 curve up to the curve with correct Pd. This abrupt rise in pressure is accompanied by an abrupt fall in velocity. Velocity is supersonic along portion of P* −6 curve involved, and is subsonic elsewhere. Dashed curves with vertical tangents are supersonic mathematical solutions that are not achieved in present nozzle configuration. *5*) Shock at outlet. Any lower value of Pd will still result in a pressure along entire P* −6 curve, if flow is steady, but will require dissipative mechanism other than steady one-dimensional shock. *6*) Exceptional curve with vanished shocks. This is the correctly expanded nozzle. *C*: downstream pressure as a function of flow rate, relates directly to *B*. *D*: flow over a rise ("constriction") in the bottom of an open hydraulic channel, bounded on the sides by planes parallel to the page. *Solid curves* represent streamlines with velocity in direction of arrows. Choke point occurs directly above top of rise, where velocity is at wave speed. Hydraulic jump to the right of rise represents a zone of dissipation of head, to achieve the imposed downstream reservoir level on the right. The intensity of dissipation of the eddies is far less than is that of viscous and conductive mechanisms in the gas shock. Hence the transition is much more gradual. *Curve W* is an example of a bottom configuration that would result in a true waterfall for low enough levels of the downstream reservoir. *E*: surfaces of water for fixed level of upstream reservoir and various levels of downstream reservoirs. Description closely follows that of *B*. *Curve 3* is the critical value of surface of water. For all downstream reservoirs level below that of *3*, the flow is limited, and only *curve 6* which has supercritical velocity downstream from the choke point will allow the possibility of a smooth transition to the downstream reservoir. Hydraulic jump, as in *curve 4* is idealized as being perfectly abrupt here, and such idealization permits calculation of a close approximation to the height at the actual jump, as shown schematically in *D* (see also Fig. 8). Transition at the jump is from supercritical velocity (or shooting flow) along a portion of *curve 6* to the subcritical velocity (or quiescent flow) approaching the downstream reservoir.

TABLE 2. *Examples of wave-speed concepts in one-dimensional flows*

	Compressible Flow	Open-Channel Hydraulics	Elastic Tube Flow
Propagating wave	Sound	Shallow water	Pulse
Energy storage	Gas compression	Water level (gravity)	Tube recoil
Wave speed	$\sqrt{\gamma P/\rho}$	$\sqrt{\rho g H/\rho} = \sqrt{gH}$	$\sqrt{Y/\rho}$
Velocity greater than wave speed	Supersonic flow	Shooting flow	Supercritical velocity
Ratio of velocity to wave speed	Mach no.	Froude no.	Speed ratio (S)
Discontinuity	Shock	Hydraulic jump	Elastic jump

H = height of liquid above bottom of channel; g = acceleration of gravity.

example, downstream from the throat of a gas nozzle a shock forms (Fig. 1, *A* and *B*), in which velocity decreases abruptly from above to below wave speed (speed of sound). The intensity and placement of the shock are such as to dissipate steadily by viscosity and heat conduction just that amount of mechanical energy needed to adjust to the downstream pressure change without affecting the upstream flow pattern. Downstream from the constriction in a hydraulic open channel, a hydraulic jump forms (Fig. 1, *D* and *E*), in which the velocity decrease from above to below wave speed (of surface disturbances) is much more gradual than is the gas shock, with the necessary energy dissipation occurring in a quasi-steady structure of eddies.

The wave-speed theory of flow limitation in elastic tubes is introduced in analogy to the constricted open channel to demonstrate the "waterfall effect" in a simple way that is closely connected to limitation in airways. Water level is the analog of cross-sectional area, each specifying the local velocity for given flow and also specifying the effective local pressure, which is the distending pressure of the tube. With this choice of pressure, the static recoil pressure is the analog of the given upstream reservoir level. An "elastic jump" is proposed as the analog of the hydraulic jump. The constriction in the elastic tube, analogous to that of the channel, is expected to occur at one of the several local minima of cross-sectional area that occur naturally along the airways.

The theoretical implications for the airway system are quantitatively developed in the frictionless case with a qualitative assessment of the effect of friction. Available experimental results are then analyzed in terms of this theory.

THEORY

Basic Aspects

To obtain a quantitative description of flow limitation during forced expiration, assumptions about the structural mechanics and fluid mechanics of the airways are specified. The airways are considered to act as if they are a single airway along which the local value of cross-sectional area varies. The value is considered to be enormous in the alveolus, to proceed to a minimum within the thorax, and then to increase as the thoracic outlet is approached, as in the Weibel data (36). Figure 2 is a schematic diagram of the airway system.

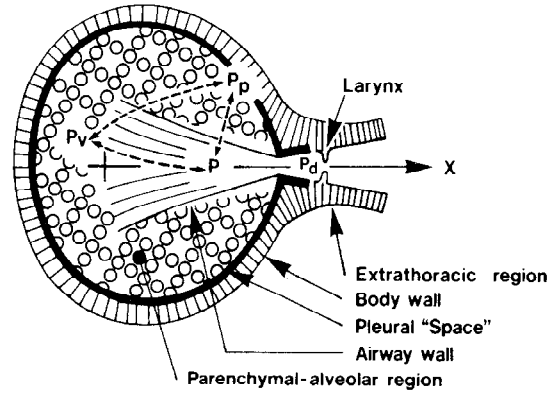

FIG. 2. Schematic diagram of symmetrical model of airway in lung. Flow to right on expiration is positive.

Another basic assumption of the modeling is that the flow is quasi-steady, meaning that no transient inertial force need be considered in the mechanics of the flow. That no time-dependent effect is necessary to produce the flow limitation phenomenon has been shown experimentally in an isovolume preparation, in which steady flow through the airways of an excised lung produced a flow limitation closely resembling that of actual forced expiration (3). The onset of forced expiration, which is effort dependent, is not considered in the present work.

General elasticity assumption. In accord with experimental observations on macroscopic airways (13, 23), the local value of cross-sectional area of the airway is assumed to be statically stable and therefore a strictly increasing function of the local distending pressure, here defined as hydrostatic pressure (also referred to as "side pressure" or simply "pressure") at a point within the airway minus the pleural pressure. Thus if we start by ignoring elastic interactions of neighboring sections of airway, the cross-sectional area is given by the function

$$A = A\ (P - Pp, X)$$

which for convenience is turned around and taken in the form that the distending pressure is the function

$$P - Pp = B(A, X) \qquad (1)$$

where B(A, X) = distending pressure function, A = area of cross section, X = distance along airway, P = local value of hydrostatic pressure, and p is the subscript indicating the pleural value.[1] The distending pressure function B(A, X) may be considered an elasticity equation of state of the airways, defined to include elastic support by surrounding parenchyma (26) without the need for direct consideration of the peribronchial pressure, which is the effective external pressure on the airway wall. The distending pressure becomes the simple transmural pressure only in the situation in which the peribronchial pressure is just equal to pleural pressure.

The local head. A very useful quantity in analyzing flows in tube systems, such as that in airways, is the head (also referred to as "total pressure" or "stagnation pressure").

[1] See section on SYMBOLS at end of main text.

$$\text{head} = P + \frac{q\rho}{2} U^2$$

where gravity is neglected in the gas flow, and where U = the average velocity in a local cross section, q = momentum correction factor for departure from a blunt velocity profile, assumed equal to one in present work, and ρ = density of fluid. According to the Bernoulli principle, this head is conserved along the tube in a frictionless flow, as long as the compressibility of the fluid is negligible, as assumed in the present work.

In the present problem the pressure and area of the airways are related according to *Eq. 1*. So if the pressure in the expression immediately above is referred to pleural pressure simply by substituting for P according to *Eq. 1*, we get a distending head, which is just the head referred to pleural pressure, a natural reference in the present problem

$$J = B(A, X) + \frac{q\rho}{2}\left(\frac{F}{A}\right)^2 \qquad (2)$$

where J = head minus pleural pressure and F = UA = volume-flow rate. For the present assumption of steady flow, the volume-flow rate was introduced because it is constant along the airway as long as gas compression is neglected, as in the present work. The distending head cannot increase in the direction of flow, without an appropriate input of mechanical energy.

With B specified as a function of A at each X, as discussed in connection with *Eq. 1*, a solution for A, and therefore B, can be determined at any point in the airway by using *Eq. 2* with any pair of values F and J. Such purely algebraic solutions will be developed and discussed below for special assumptions on the airway elasticity. First, however, it is instructive to derive the condition for maximum flow. This critical condition governs flow limitation.

Critical Condition

Equation 2 is readily solved for F to examine its possible range of values as a function of A and X

$$F(A, X) = \left(\frac{2}{q\rho}\right)^{1/2} (J - B)^{1/2} A \qquad (3)$$

Examples of the area dependence of this function for fixed J are shown in Fig. 3*B*. At each point X along the airway this function will have a maximum possible value as a function of A. First consider the basic case in which the area dependence of B is such that $\partial F/\partial A = 0$ for fixed J holds at only one value of A. At that value of A

$$\frac{\partial F}{\partial A} = \left(\frac{2}{q\rho}\right)^{1/2} \left\{ -\tfrac{1}{2} (J - B)^{-1/2} \frac{\partial B}{\partial A} A + (J - B)^{1/2} \right\} = 0$$

or

$$J = B + \tfrac{1}{2}Y \qquad (4)$$

where $Y = A\partial B/\partial A$ = elastic modulus (reciprocal of specific compliance) of the airway cross section. An example of this relationship is plotted in Fig. 3*A*. A key

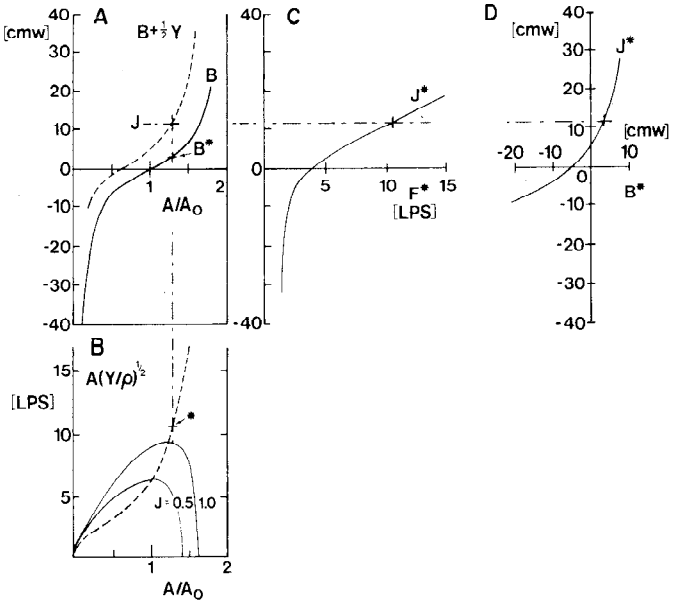

FIG. 3. Relationships among variables at the choke point, constructed on the basis of the Fry form of distending pressure function B as in *Eq. 7* with Yo = 10 cmH_2O, Ao = $2cm^2$, Au/Ao = 2, and ρ = 1 g/l. *A*: distending pressure (—) and critical value of distending head (– –), both as a function of the area ratio, A/Ao (see also Fig. 7*A*). A specified distending head J* at the choke point specifies A* and B*. *B*: physically achievable flow rates for specified head (—) and locus of maximum possible flow rate (– –), both as a function of area of the cross-section. A* specified in *A* specifies the maximum flow rate, $A^*(Y^*/\rho)^{1/2}$, provided it has the lowest value occurring along the tube. *C*: distending head at the choke point versus (actual) critical flow rate, a cross plot of *A* and *B*. *D*: distending head and pressure at the choke point, a cross plot from *A*.

expression for the maximum possible steady flow rate at the point X under these conditions is obtained by substituting into *Eq. 3* the expression for J – B according to *Eq. 4*, giving

$$F = A(Y/q\rho)^{1/2} \qquad (5)$$

where $(Y/q\rho)^{1/2}$ is the speed of pressure wave propagation. This relationship between the maximum possible flow rate and the local cross-sectional area is shown in Fig. 3*B*, which shows a strictly increasing function of A in this case. *Equations 4* and *5*, or equivalently Fig. 3, *A* and *B*, together give the relationship between head and the maximum possible flow rate at each cross section, yielding the result of Fig. 3*C*. Now the *minimum* value in X (along the airway) of this local maximum possible flow rate for given head is the prediction of the *actual maximum steady flow rate*, called here the critical flow rate[2]

$$F^* = A^*(Y^*/q\rho)^{1/2} = A^* U^* \qquad (6)$$

where $U^* = (Y^*/q\rho)^{1/2}$ = wave speed; and where * (read star) is the superscript to indicate value at this critical (mini-max) point (Ar, Xk), r is the subscript to indicate the critical value associated with the actual maximum steady flow rate, and k is the subscript to indicate the

[2] Taking account of compressibility of the fluid requires a modified Bernoulli principle (32) and a strict mass conservation to derive the appropriate critical condition. The resulting modified wave speed is as in *Eq. A-1*.

critical (or choke point) location. According to this result for critical (or actual maximum) flow rate, *Eqs. 4* and *5* hold only at the choke point, where the variables all have stars. The critical distending pressure that corresponds to Fig. 3, *A–C*, is of interest in applications and is plotted in Fig. 3*D*. It should be appreciated from the above development that a specified B(A, Xk) completely determines the relationship between F* and J* for a specified $q\rho$ (see APPENDIX C, in which the reverse is also demonstrated).

The derivation of the wave-speed criterion on flow limitation in elastic tubes (*Eq. 6*) depended principally on a locally defined head and the elastic recoil of tube wall. The implication is that, whatever the friction, limitation occurs if flow is increased to such an extent that the Bernoulli effect results in a cross-sectional area sufficiently small that the velocity at that area is at wave speed.

Equation 5 is essentially equivalent to the theoretical slope conditions on flow limitation in the work of Lambert and Wilson (20) and Pardaens et al. (30), which was translated directly into calculus conditions by Clément et al. (2) and in a related context by Pederson (31), although none of these works considered wave speed explicitly. It can also be shown that the wave-speed condition of *Eq. 6* is satisfied by Fry's theoretical prediction of maximum flow in a uniform tube with frictional loss (7).

Figure 3 provides a graphical basis for describing the elastic determinants of the critical flow rate. The B(A) curve (Fig. 3*A*) that has the smallest area for a given distending pressure will tend to result in the lowest flow rate (Fig. 3*B*). So the choke point will tend to occur at such a "constriction." The magnitude of the curve of $AY^{1/2}$ at that choke point then determines the flow rate for a given head (Fig. 3*C*). As a simple example of these considerations, let a constant Bc be added to B(A, X) (30), implying a reduction of area at each distending pressure. From *Eq. 4* or the construction of Fig. 3 the effect at constant J is seen to be a reduction of A* equivalent to reducing J by the amount Bc while retaining the original B(A, X). This example holds whether considering one location compared to another as a potential choke point or considering alteration of the properties at a given choke point to determine a new flow rate.

In examining the range of values of F(A, X), as in *Eq. 3* at the beginning of this section, the other important case to consider is that of $\partial F/\partial A = 0$ for two values of A. This case occurs if $AY^{1/2}$ decreases with A to a minimum value and then increases for high values of A. This is a tube, postulated by J. Mead (personal communication), that has a flow limitation at high enough values of A, where $\partial F/\partial A = 0$ identifies a local maximum of F as a function of A, but becomes too stiff to limit at low values of A, at which $\partial F/\partial A = 0$ identifies a local *minimum* of F as a function of A.

Frictionless Example

With the critical conditions of the flow in the airway established, solutions of *Eq. 2* are now obtained to provide theoretical predictions of the variation of distending pressure along the airway for steady flows. For simplicity and to emphasize that ordinary tube friction is in no way necessary in the present theory of flow limitation, it is assumed that the flow is essentially frictionless along the tube system from the alveolus at least up to the choke point. As indicated above, the assumption of frictionless flow, or no head loss, implies that at all points upstream from the jump, the distending head is equal in value to the static recoil pressure of the lung

$$J = Bv = Pv - Pp$$

where the subscript v indicates alveolar value. The effect of friction, which is not expected to be great except at low lung volumes, is qualitatively assessed as a head loss, a reduction of J below Bv. So for example, the frictionless prediction of MFSR curves furnishes an upper bound on actual lung curves.

Fry's form for area dependence. A form of area dependence of the distending pressure function, which characterizes the airways over a large range of distending pressures, is that of Fry (8). This form has also been used by Pardaens et al. (30). It is written here so as to emphasize the reference or resting (B = 0) condition and the upper asymptote on area

$$B(A/Ao;\ Au/Ao,\ Yo) = Yo \cdot \left[1 - \frac{Ao}{Au}\right]\left[-\frac{Ao}{A} + \frac{1 - Ao/Au}{1 - A/Au}\right] \quad (7)$$

where u is the subscript indicating the local value of the upper asymptote and o is the reference subscript indicating here the local value for zero distending pressure. This relationship has B strictly increasing ("sigmoidally") with A from negative infinity at the lower asymptote, A = 0, to positive infinity at the upper asymptote, A = Au. The parameters displayed in *Eq. 7* explicitly represent the asymptote Au as well as the reference area Ao at the zero-pressure crossing and the elastic modulus there (see Fig. 3*A* for a plot of a representative pressure-area relationship). The reference state, B = 0, is by definition the state at which (hydrostatic) pressure in the airway equals pleural pressure. In an actual lung, this state is achieved statically for intraparenchymal airways only by a special technique, such as that of Takishima et al. (35), in which beads are used to seal the airways off from the alveolus. Dynamically the reference state is achieved only at an equal pressure point (EPP).

The present assumptions on the parameters of the distending pressure function are *1*) Ao, the reference area decreases along the airway from its very large alveolar value to a minimum value (Aok) and increases from this minimum to the thoracic outlet; *2*) Yo, the reference value of elastic modulus is constant along the airway (Yo = Yok); and *3*) Au/Ao, the ratio of the upper asymptotic area to the reference area is constant along the airway.

Variables used in plots. For these assumptions the results of solving *Eq. 2* are shown in Fig. 4, where the

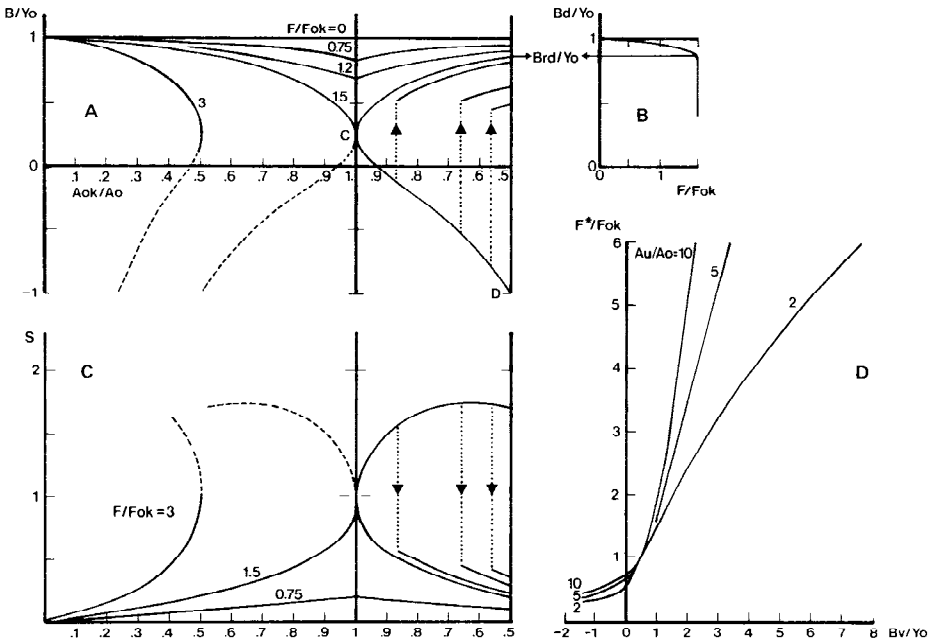

FIG. 4. Frictionless results with Fry form for area dependence at distending pressure function. *A*: distending pressure ratio as a function of location, which is expressed as a reciprocal of reference area. Alveolar region is at the left-hand edge of the plot, and the choke point of the full airway system is at the vertical line, Aok/Ao = 1. Elastic jumps are represented as the vertical dotted lines to the right of choke point, where Aok/Ao is decreasing in the direction of flow. Arrows indicate direction of transition from upstream to downstream branch of solution curve. Dashed portions of solution curves are physically unrealizable in the present context. *B*: downstream distending pressure ratio as a function of speed parameter for the conditions of *A*. *C*: velocity ratio, local flow velocity divided by local wave speed as a function of location, plotted as in *A*. Note that the only realizable branch with S > 1 is CD, which provides a smooth transition from velocities less than to velocities greater than wave speed. *D*: speed parameter as a function of static recoil pressure ratio for specified values of Auk/Aok.

parameters and variables are expressed as ratios in order to enhance the versatility of each plot. New definitions are $S = U/(Y/q\rho)^{1/2}$ = ratio of local velocity to the local wave speed at a cross section; $Fo = Ao(Yo/q\rho)^{1/2}$ = flow rate that would occur if the velocity at that location were equal to the wave speed of the reference cross section there; and where d is the subscript indicating the downstream location at the thoracic outlet. The dimensionless variable S is the analog of better known ratios of flow velocity to speed of propagation of pressure disturbances: the Froude number for flow velocity relative to speed of surface waves in shallow water and the Mach number for flow velocity relative to speed of sound waves in a compressible fluid. Note that $S^* = 1$. An alternate form for this variable is

$$S = F/\{A(Y/q\rho)^{1/2}\}$$

emphasizing the reciprocal relationship to the variable $AY^{1/2}$.

The construction of Fig. 4*A* is described in APPENDIX B. In Fig. 4*A* distending pressure (divided by the constant elastic modulus Yo) is plotted against the variable Aok/Ao which indicates location in the following manner: the decrease of Ao from its essentially infinite value near the alveolus to its minimum value Aok corresponds to the increase of Aok/Ao from zero to unity shown in the left-hand portion of the plot. The increase of Ao from its minimum value to the assumed value (2Aok) at the thoracic outlet downstream corresponds to the decrease of Aok/Ao to one-half in the right-hand portion of the plot. The use of the symbol Aok for the minimum value of Ao is only justified by the fact that for the present simple assumptions on elasticity and the assumption of frictionless flow, the choke point is located at the minimum of the reference area function Ao(X). Figure 4*C* is a companion plot showing the ratio of flow velocity to wave speed and is constructed from cross-sectional areas implied in Fig. 4*A*. In both these plots the horizontal scale is readily transformed to X for a given Ao(X). Only when Ao-Aok is proportional to $|X - Xk|$ is the shape of the plots shown the same as the plots against X. In the more typical circumstance of a smooth variation of reference area, (Ao − Aok) is proportional to $(X - Xk)^2$, and the slope of the curves of B (or A) as a function of X remains finite, even at the choke point (see also Fig. 10*B*).

Resulting solutions. As in the compressible-flow and open-channel analogies, the plot of B/Yo for a fixed upstream value, Bv, shows a difference in character according to whether the downstream value, Bd, is above or below a critical value, Brd (see Fig. 4, *A* and *B*). If Bd is not below this critical value, then the curves corresponding to a decrease of Bd below Bv have increasing values of flow parameter F/Fok, and therefore flow rate. There is an accompanying increase in the depth of the dip in the curves showing the variation of distending pressure with location. The critical value of Bd occurs for flow velocity reaching wave speed at the bottom of the dip. No further increase of flow takes place for any decrease of Bd below critical, and the flow is choked or limited. The effect of further decrease of downstream pressure is predicted to require—in viola-

tion of the assumption of frictionless flow—a head loss, idealized as an "elastic jump" occuring at a single point, as shown in APPENDIX B. This jump is *from* the curve which connects the choke point C and the downstream point D. All velocities on this curve (except *at* C) are greater than wave speed, as shown in the companion Fig. 4*C*. The jump is *to* the curve that connects to Bd without friction. All velocities on this curve are less than wave speed. For all negative values of Bd, there is only one EPP, and it is located downstream from the choke point in the present example.

In practice, just as in the hydraulic jump, the flow downstream from the choke point should be expected to be complicated. Wall friction should be of importance in the section of high velocity just downstream from the choke point. Instead of the idealized abrupt elastic jump of Fig. 4*A* from one frictionless solution to another, an extended transition with standing eddies resulting from the flow separation is expected to occur. Nevertheless, the key feature of the transition, the head loss necessary to maintain steady flow, is calculated from the simple discontinuity. In analogy to the constricted channel (1), the velocity upstream from the jump is assumed to be essentially stable and steady,[3] as long as the downstream pressure is not so low as to cause the jump to reach the exit of the elastic tube system. For lower downstream pressures, the question of a mechanism to dissipate sufficient head arises, and it is probable that a highly unsteady flow is required (12). Unsteady limited flows are readily observed in elastic tubes (7).

Figure 4*B* shows a plot of the variation of Bd with the flow ratio F/Fok, as constructed from Fig. 4*A*. The flow increases with decreasing distending pressure Bd up to the limiting flow plateau. The curve is for the fixed upstream (alveolar) distending pressure or static recoil. So it is essentially a prediction of a family of isovolume-pressure-flow (IVPF) curves of the excised lung, for which Pd = 0 so that Pp = −Bd. For the lung in situ the pressure drop Pd of the extrathoracic airway must be added to the negative of Bd to obtain pleural pressure: Pp = Pd − Bd, by virtue of *Eq. 1*.

In Fig. 4*D* each curve is the plot of critical value of flow parameter F*/Fok against the static recoil condition upstream, Bv/Yok, for the specified value of Au/Ao. Separate curves like those of Fig. 3, *A* and *B*, were required for each value of Au/Ao. The result gives that part of the maximum-flow static recoil (MFSR) curve which is at high enough lung volumes that the flow can be considered frictionless and over a narrow enough range of lung volumes that the parameters, Yok and Auk/Aok, can be considered constant. It is important to note that this result does not depend on any airway property except at the choke point, in contrast to the local variations of Fig. 4, *A* and *C*, which do depend on the assumptions of constancy of Au/Ao and of Yo along the airways. In the case of nonnegligible friction, the predicted MFSR curve does depend upon the properties along the airway. The general qualitative effect of friction is to shift points on the frictionless MFSR curve to the right by the amount of head loss from alveolus to choke point, an amount that depends on flow rate (see also the section on qualitative effect of friction).

Figure 4*D* implies that the critical flow rate F* is proportional to Aok and to $\rho^{-1/2}$ and increases with the static recoil Bv. The dependence on Yok is less obvious because that physical quantity is in the scaling of both coordinate axes. To unravel this dependence numerically requires further computation, but the direction of the change in critical flow rate with Yok can be argued physically. Consider a stiffening of the airway wall in the sense of increasing Yok in the two possible inflation conditions: positive values and negative values of B*. In both conditions the stiffening tends to change the area A* toward the reference state Aok. For positive distending pressures this increased stiffness results in a decreased area A* and a decreased critical rate of flow. For negative distending pressures the increased stiffness results in an increased area A* and an increased critical rate of flow. The overall result that an increase of Yok has on the MFSR curve is decreased slopes at all values of recoil pressure.

Further Aspects of the Theory

The above theoretical results provide a useful context for further developments. The frictionless analysis is readily extended to include other forms of area dependence of distending pressure. The power-law form, which is especially instructive, is developed below. The case of a discontinuous shift of location of choke point is explained. Then, before considering experiments on real lungs, there is discussion of important ways in which the present modelling assumptions require modification: consideration of friction, of longitudinal tension, and of uncqual branchings.

Power-law form for area dependence. The assumption of power-law form for area dependence of the distending pressure function is appropriate over limited ranges of that function and permits simple algebraic development of critical flow relationships, as in APPENDIX C. The assumed power-law form of area dependence at the choke point is taken to be the increasing real function

$$A = Z[n(B - Bo)]^{1/n} \qquad (8)$$

where the following are real numbers n = an index (≥ -2), Z = constant of proportionality = $Z_1^{-1/n}$ of APPENDIX C, Bo = reference value of pressure, in which o is the reference subscript used here for states A = 0 (n > 0) and A = ∞ (n < 0), in contrast to previous reference state, B = 0. The constant of proportionality, Z, is the tube area compliance (reciprocal elastance) for n = 1 and can be interpreted analogously for n ≠ 1. For tubes such as the larger airways, in which a (real positive)

[3] R. T. Jones (18) argued that velocities above wave speed would necessarily be unstable in a uniform tube, and Pardaens et al. (30), without using the concept of wave speed, argued similarly to arrive at a maximum flow rate through the tube system. These arguments, however, do not establish that flows with velocities greater than wave speeds are necessarily unstable, even in uniform tubes, because they fail to take account of the disappearance of the disturbance by wave propagation along the tube. Steady flows with velocities greater than wave speed are readily produced in uniform open channels (1, 32), and a likely interpretation of Griffiths' experiments is that flow velocities greater than the wave speed were readily obtained in the uniform rubber tube (11).

area exists for B = 0, the two fundamental constants Z and Bo are expressed in terms of the two reference values, Ao, Yo, in *Eqs. C-6* and *C-7*.

The area dependence of *Eq. 8* implies a specific power-law relationship between head and critical rate of flow

$$F^* = W[m(J^* - Bok)]^{1/m} \quad (9)$$

where

$$m = 2n/(2 + n) \leq 2 \quad (10a)$$

$$W = (q\rho)^{-1/2}\, Zk \quad (10b)$$

and in terms of the case of reference state, B = 0

$$W = (q\rho)^{-1/2}\, Yok^{-1/n}\, Aok \quad (11)$$

The dependence of critical flow rate on density, head, reference pressure, and the constant Z is clear from *Eqs. 9* and *10*. Similarly, the use of the parameterization with Aok and Yok shows directly the dependence of critical flow rate on Aok. The dependence on Yok is obtained by differentiation, and it is found, as can be shown quite generally for that form of parameterization, that F* increases with Yok for B < 0 but decreases for B > 0.

Not only does *Eq. 8* imply *Eq. 9* but the reverse is also true. Examples of this correspondence are shown in Fig. 9, *A* and *B*. To explore this correspondence further a particular simple frictionless example is chosen so that *Eq. 9* becomes the MFSR relation. It is assumed in *Eq. 8* that for negative values of Bk, an inverse proportionality holds, n = −1, and for positive values of Bk the square law holds, n = 2. These two portions of the area dependence are assumed to join smoothly. The corresponding powers for the MFSR relationship are m = −2, m = 1. For representative values of Aok and Yok these two relationships are shown in the solid curves of Fig. 5, *A* and *B*. These are constructed from Fig. 9, in which it may be observed that the general character of both area dependence and MFSR curve is similar except that as n ranges upward from −2 to ∞, m ranges upward from −∞ to 2, with the special case, n = m = 0. Limiting points, Bok, of corresponding curves are identical. As a particular example the area dependence for n = 2, which is concave downward, corresponds to an MFSR curve which is straight, m = 1.

An MEFV curve that corresponds in turn to the above MFSR relationship is obtained by applying a standard pressure-volume curve to the MFSR curve. The result is as shown in Fig. 5*C*. It is emphasized that these predictions of MFSR and MEFV curves are based on the assumption that Yok is independent of lung volume, an assumption made in effect by Pardaens et al. in their predictions which included frictional effects and were based on the Fry form of area dependence (30). See the DISCUSSION below for the effect that a more realistic assumption about dependence of Yok on lung volume has on the MFSR and MEFV curves.

The power-law assumption leads to a simple expression, *Eq. C-13*, for the ratio of reference cross-sectional area at the choke point to area at the EPP. A related result of APPENDIX C, which is true for any area dependence and is important in experimental applications below, is that for a sufficiently negative downstream pressure the cross-sectional area at the EPP is greater than or less than that at the EPP according as F*/Fok is greater or less than one, or equivalently, according as J*/Yok is greater than or less than one-half.

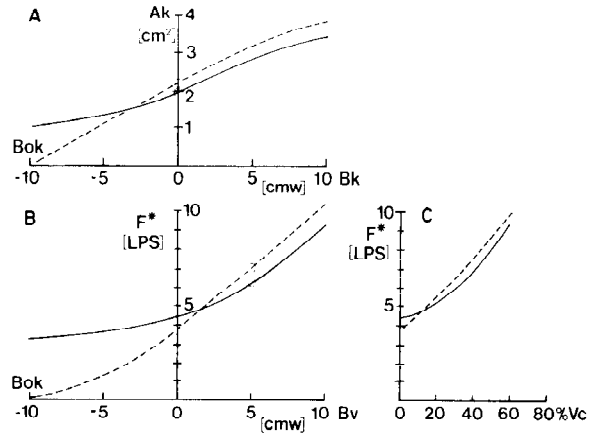

FIG. 5. Composite power-law form of area dependence of distending pressure curves and corresponding critical flow curves in the frictionless case. All curves are for Yo = 10 cmH_2O. *Solid curves* (—) are for Ao = 2 cm^2, with n = −1 for Bk < 0 and n = 2 for Bk > 0. *Dashed curves* (– –) are for Ao = 2.2 cm^2, with n = 1 for Bk < 0 and n = 2 for Bk > 0. Circled point indicated break in the power law forms. *A*: cross-sectional area as a function of distending pressure. *B*: maximum possible rate of flow (ρ = 1 g/l) through locations Xk, as function of recoil pressure and *C*, as a function of percent of VC, based on pressure volume curve of Fig. 6*C*. Actual critical flow rate is the lower of the two maximum possible rates and the choke point location is determined accordingly. At the intersection of dashed and solid curves in *B* and *C* both points can be considered choke points. In *A* and *B* the intercepts Bok for A = 0 and F = 0 are indicated in the case in which they occur.

Discontinuous change of location of the choke point. Finding the minimum value of $AY^{1/2}$ along the airways, for each recoil pressure in the frictionless case, gives both the value of critical flow rate and the corresponding location of the choke point. In the power-law situation, consider two locations that are local minima of $AY^{1/2}$ along the airway. Suppose that one location has a distending pressure relationship and an $AY^{1/2}$ as in the solid curves of Fig. 5, *A* and *B*, and the other, as in the dashed curves. The resulting MFSR curve and MEFV curve is then the lowest of the two curves in Fig. 5, *B* and *C*. The location of the choke point corresponds to the curve from which flow is actually predicted.

Qualitative effect of friction. The primary effect of simple wall friction along the airway is to make the pressure gradient more negative than without friction so that negative gradients become steeper and positive gradients less steep. Overall pressure drops are thus increased, resulting in decreased rates of critical flow because the function $A(Y/q\rho)^{1/2}$ must decrease with decreasing area to produce limitation, and consequently the critical flow rate decreases with decreasing distending pressure (see Fig. 3). A more physical way of looking at this decrease of critical flow with friction is that friction causes the local (distending) head at the choke point to be reduced below the static recoil value, and this reduced local head, which governs the choking, implies a reduced critical cross section, resulting in a

reduced critical flow. Thus in Fig. 4*D* the effect of friction is to shift points of the MFSR curve to the right because the actual value of static recoil pressure must be greater than the value of the distending head at the choke point (see also *Eq. 9* for a simple formula for the effect).

Even a small frictional effect modifies somewhat the simple frictionless situation in which critical rate of flow is determined only by elastic recoil, gas density, and the pressure-area relationship at the choke point. For sufficiently great frictional effect the gas inertia becomes negligible in setting the critical rate of flow. In this situation the critical rate is set by the condition that the frictional-elastic interaction along the airway results in an airway that is virtually closed at some point. At that point the inertial-elastic interaction, represented by the wave-speed criterion, predominates so that the airway stays open with an appropriate small area for the critical rate of flow.

Complications at the choke point. The flow approaching a choke point is converging (decreasing cross section) and will tend to be blunt and therefore rather well characterized by the present quasi-one-dimensional analysis in the segment upstream from the choke point, which segment is the one that matters in setting the flow limitation. The difficulty comes in the elastic description of the collapsible tube. If there were no elastic interaction between successive cross sections along the tube, then the theory would be strictly predictive in terms of a pressure-area function that is independent of variation of area of cross sections that are neighboring the choke point. However, the effect of longitudinal tension in the tube walls, and its equivalent in the attached parenchyma can modify the area dependence of the distending pressure function of the tube in two ways. One results in a general decrease of critical flow rate due to a circumferential contraction through Poisson's ratio. The other results in a decrease of flow rate as effort increases above the critical value because of a marked change of effective curvature $\partial^2 A^{1/2}/\partial X^2$ as the elastic jump moves downstream from the choke point. The flow separation that is most likely to occur in an expanding section of airway, for downstream pressures that are just critical (Bd = Brd), appears to further complicate this effect of longitudinal tension. A preliminary theory that predicts the effect of longitudinal tension has been developed by T. Wilson (personal communication) and by Griffiths (12).

Heterogeneous pathways. Although the present theory is developed essentially for a uniformly branching model of an airway, equivalent to a single pathway, the actual lung airways branch asymmetrically, suggesting the need to consider a heterogeneous effect. Even if the heterogeneous effect is substantial, as can be expected at low lung volumes and in disease, the present concept with different choke points in different pathways can be used to analyze the problem on the basis of the character of the heterogeneity. However, such an analysis is probably best done in close connection with experiments and is not considered further in the present work.

APPLICATIONS TO EXPERIMENTS

In view of the central role proposed for the choke point in elastic tubes, we interpret available experiments that relate to choke point considerations. Some of our own experiments to locate the choke point and to check the critical conditions in isolated airway preparations are summarized (5, 6). Then the key problem of locating the choke point in actual lungs is pursued on the basis of reports of airway conditions during flow limitation. The analysis in terms of the present theory is indirect because of the absence in these reports of any direct determination of choke point or of a sufficient determination of airway dimensions and elasticity, from which the choke point and critical rate of flow could be decisively determined. These reports were of the two studies on dog lungs by J. G. Jones et al. (16, 17), called here Jones I and Jones II, and of three studies on dogs and humans by Macklem and co-workers (10, 21, 22). An important factor in all these analyses is the relationship of lung volume to properties at the choke point.

These experiments on lungs were also reviewed from another perspective: to assess the extent to which friction could be ignored in predicting the expiratory flow limitation. The inclusion of friction is a complicating feature of the analysis because it requires consideration of airway properties at points upstream from the choke point. These properties, which depend strongly upon the lung volume, are generally not well known.

The Choke Point

Experiments on isolated airways. The basic wave-speed condition of flow limitation was tested in a series of experiments on isolated "airways" (5, 6). These controlled experiments illuminated some of the difficulties and indicated some useful approaches to locating the choke point as well as to evaluating the properties there.

The "airways" tested were *a*) excised dog tracheas and *b*) a tube with rigid, open semicircular cross section, the open length of which was covered by a rubber membrane. In this design to mimic the trachea, the rubber avoided the substantial effects of tissue fatigue inevitable in the biological preparation (25). The choke point was located by tracing the locus of the minimum value of distending pressure as the downstream distending pressure was reduced below upstream distending pressure, which was held constant. At the onset of flow limitation, the abrupt downstream turning of the locus of the minimum values of B, as the elastic jumps formed, was used as the estimate of the location of the choke point, at which the cross-sectional area was measured.

An important result was that within about 10%, well within experimental uncertainty, the critical condition was verified as long as the evaluation of Y was made directly at the critical flow condition so as to include the effect of longitudinal tension. Evaluation of Y from the static pressure-area characteristic without correction led to some substantial discrepancies. This finding has importance in making accurate theoretical predictions of critical flow for the lung as mentioned in the theory section above.

Negative effort dependence. An example of the importance of longitudinal tension is offered in an explanation of the phenomenon of negative effort dependence as

an extension of the present theory. In some lungs it is found that with increasing effort at a given volume the forced expiratory flow rate declines somewhat from a peak value, eventually appearing to reach an asymptote at very high effort (large pleural pressure, corresponding to very negative values of Bd). Such negative effort dependence has been displayed graphically in isovolume-pressure-flow curves (9) and is exhibited in flow-volume curves of Jones II.

A qualitative theoretical explanation is based on the general idea, expressed independently by J. Mead (personal communication) and one author (*EE*), of how longitudinal tension effects the area dependence of the distending pressure function at the choke point. The contribution of longitudinal tension to distending pressure is equal to the negative of the product of the curvature $\partial^2 A^{1/2}/\partial X^2$, a numerical shape factor, and the tension. Thus Bk is decreased by positive curvatures, as are expected at Xk for critical value of downstream pressure, Brd. Then according to Fig. 4*A*, A* will be increased by the positive curvature, and so would $(AY^{1/2})^*$ or W of *Eq. 9* tend to be increased. But as Bd is made more negative than Brd (increased effort), the curvature at Xk would be greatly reduced. Hence, any increase of $(AY^{1/2})^*$ or W would be lost, and the resulting critical rate of flow would be reduced as pleural pressure is increased somewhat above the critical level.

Indirect evidence on choke points. In a study of limitation of flow from excised dog lungs, Jones I reports distending pressures and cross-sectional areas of airways that permit some interpretation by the present theory. In their Fig. 8, the ratio of cross-sectional area to the maximum value is plotted as a function of lung volume for three locations—the first near the tracheal outlet, the second near the carina, and the third in mid-main bronchus—at each of two different driving pressures (Bd). At the more negative value of Bd, the area ratio near the tracheal outlet decreased markedly for increasingly negative Bd, consistent with a location downstream from the choke point, which location passed from being downstream from the elastic jump to being upstream as Bd became more negative. The area ratio near the carina decreased little for increasingly negative Bd, except at low lung volume, at which a marked decrease did occur. This situation is interpreted as a location upstream from the choke point except for the low lung volume at which the choke point shifted its location upstream from the carina. The mid-main bronchus did not change area with Bd, indicating a location upstream from the choke point at all lung volumes.

The flow-volume curve for this study was of the type with a near plateau of flow for the middle range of lung volume, and with a sharp drop in flow at low lung volumes. This abrupt change of character of the curve is consistent with the shift of choke point from a stiffer to a less stiff airway as discussed in the theoretical section. The constancy of flow rate on the plateau is consistent with their measurements of area dependence of distending pressure being near to a power law with $n \simeq -2$ and Bok $\simeq 0$, according to the present theory and also as pointed out in their analysis.

Another of the results of Jones I, which can be interpreted by the present theory, is the observed variation in pressure and head along the airway during forced expiration at mid-lung volume (their Fig. 7). An observed minimum of cross-sectional area along the airway, about 5 cm from the tracheal outlet, corresponded to the inflection point of the curve of B(X), as would be consistent with the location of a choke point. There was also a marked head loss in a zone downstream from this point, as would be associated with an elastic jump.

In Jones II the influence of tracheal properties was studied by several interventions: stiffening by insertion of rigid tubes and by use of a smooth-muscle constricting agent and weakening by digestion with an enzyme. Both types of stiffening resulted in higher flow rates at greater than mid-lung volumes, reduced flow rates for a range of lung volume below midvolumes, and coincident flow rates at low lung volumes. The increased flow rates for the stiffened tracheas are consistent with the interpretation that the value of $AY^{1/2}$ was increased at the choke point. The reduced flow rate is interpreted as being due to the shift of the choke point from the stiff trachea to a less stiff upstream airway at a higher lung volume than normal, thus causing a premature drop from the flow plateau. The sudden drop in maximum flow both in these lungs with stiffened trachea and in normal lungs is interpreted as resulting from marked negative effort dependence due to the effect of longitudinal tension at the upstream choke point.

Choke point inferred from EPP. The above interpretations of the plateau-and-drop form of MEFV curve of Jones I are consistent with an analysis of the observed movement of the EPP. Over the range of lung volumes of the flow plateau, the EPP moved from 7 cm upstream from the tracheal outlet to 24 cm upstream (2-mm airways). The decrease of recoil pressure was accompanied by a decrease of distending pressure all along the airway, resulting in the observed movement of EPP upstream from the inferred stationary location of the choke point. For the narrow range of lung volumes of the sharp drop in flow rate, the EPP moved from 24 cm upstream from the tracheal outlet to 19 cm upstream. The static recoil pressure decreased only a little and the frictional and inertial pressure drop sharply decreased with the sharp decrease in flow rate, resulting in the observed downstream movement of EPP. At lowest lung volumes the EPP again moved upstream. The flow rate was no longer changing greatly and the decrease of distending pressure again resulted in the upstream movement.

The experiments of Mead and Macklem included dog lungs that were studied both in the chest and then after excision. Only one MEFV curve (*dog 3*, excised) had the extreme plateau and sharp drop reported in Jones I. However, all of the MEFV curves in the excised state had sharp bends (knees), and *dog 5* (excised) had an EPP locus with the broad features reported by Jones I. Except for one lung (*dog 7*) out of six that were reported, removal from the chest had a substantial effect, tending to produce a more distinct bend on the MEFV curve and tending to shift the EPP locus upstream by several centimeters, generally to the carina, over the range of lung volumes of 30–80% VC. At those lung volumes in intact lungs, the EPP was not more than 6 cm upstream from the carina, generally corresponding

to being no further peripheral than lobar bronchi, which are only partly in the parenchyma. At lower lung volumes there was a pronounced upstream movement of EPP for decreasing lung volume, as was explored further in later work (10).

The fixed EPP is readily interpreted as being near a fixed choke point that is associated with a substantial dip in the static value of $AY^{1/2}$ as a function of length along the airway. This dip then produces a pressure-distance curve along the airway which is very steep in the vicinity of the choke point, making it possible for the EPP to stay so close to the choke point as to appear fixed as lung volume is decreased. Such steep pressure gradients which include an EPP have been observed in a normal human at the carina (F. Hoppin and J. Mead, personal communication) and in the isovolume preparation with an excised dog lung (J. Friend, personal communication). The peripheral movement of EPP, as mentioned above in connection with the description of Jones I, could then be due either to an extraparenchymal location of choke point with a very gentle pressure gradient in its vicinity or to progressive upstream movement of the choke point into the parenchyma as the elastic support of the parenchyma is decreased with decreasing lung volume.

Macklem and Mead also give loci of EPP for three excised human lungs. In one the EPP remained near the carina for 80%–50% VC, while the other two were nearly fixed 5–6 cm upstream from the carina for that range of lung volume. All three of these fixed extraparenchymal loci of EPP are also expected to be approximate loci of the choke point, by the arguments just given for the dog. In an early bronchial catheter study in normal human subjects, Macklem and Wilson located the EPP over the range of lung volume 25–75% in a segmental bronchus. Some of the detailed measurements are given for one subject (*JH*). The large frictional loss that would account for the EPP being so far upstream at that lung volume was also directly observed in their Fig. 6. This large frictional loss may well be due to a reflex bronchoconstriction induced by the catheter and possibly acting only in that one pathway. Such a constriction is consistent with later observations of an upstream shift of EPP by vagal stimulation in dogs with open chest and of downstream shift by vagotomy (10). In any case this fixed location of EPP is strongly suggestive of a choke point occurring in the vicinity of that EPP.

Indications of Friction

Measurements of frictional loss reported in the above studies are examined here in order to indicate that the frictionless analysis may often apply in making accurate predictions of critical flow for a wide range of lung volumes in dogs but not in humans. The qualitative effect of large frictional increases due to bronchoconstriction is mentioned. Finally a study of density dependence of critical flow is mentioned in order to indicate the importance of friction at low lung volumes in humans.

Measurement of friction loss. The data of Macklem and Mead can be used to reconstruct the head (frictional) loss from alveolus to EPP in dog lungs (21). From their Figs. 4 and 10 this head loss is seen to average about 1 cmH_2O in vivo over the range of lung volumes 25%–70% VC, but in excised lungs the average rises from 1 cmH_2O at 25% to 3 cmH_2O at 70% VC. In individual lungs in vivo, however, reference to their Figs. 5 and 8 shows a value as high as 2 cmH_2O at 25% in one dog (*no. 8*) and values as high as 2 cmH_2O at 70% VC in two dogs (*no. 5* and *6*). In these dogs the choke point was located by the above interpretation near the fixed EPP down to 30% VC; so the head losses to the EPP are also to the choke point over most of the range 70% to 30% VC. Thus, over this range of lung volumes, the head is reduced 1 cmH_2O or sometimes 2 cmH_2O below the static recoil values of 2–8 cmH_2O over that range. The effect that this amount of head loss has on predictions of critical flow rate is just that of an equal loss of elastic recoil, shifting points on the MFSR curve to slightly higher values of pressure.

In the excised lungs of that study there was substantially more friction. In the study on excised dog lungs by Jones I, in which the above interpretation was that the EPP was progressing well upstream from the choke point for a large range of lung volumes there was reported a substantial loss of head. At a point just downstream from the apparent choke point the distending head was found to be from -5 to $+2$ cmH_2O for the large range of lung volumes of the flow plateau (75% to 25% EV). In these circumstances the frictionless analysis is less likely to be accurate.

The head loss in humans from alveolus to EPP has been reported to be substantial for critical flow. Macklem and Mead (21) reported in their Fig. 9 a substantial loss in three excised human lungs, on the order of 10 cmH_2O over the range 70% to 30% VC. These were cases in which the above interpretation was that the EPP was near the choke point, so this is an estimate of loss to the choke point. Previously, Macklem and Wilson (22) reported in their Fig. 7 a head loss rising from 4 to 7 cmH_2O to the EPP in the segmental bronchus of catheterized airways in human subjects for lung volumes from 25% to 75% VC. Such large head losses would appear to make the frictionless analysis inaccurate.

In a study of normal human subjects by purely noninvasive methods, Mead et al. reported results consistent with the frictionless assumption at high lung volumes (27). The maximum effort-independent flow rate and static recoil pressure at that lung volume were used to compute the area at the EPP. This value of area was then found to be close to (but generally greater than) the X-ray measurement of tracheal cross section at RV. However, as Macklem and Mead pointed out, the results are also consistent with a substantially larger value of area at the EPP and a substantial head loss to the EPP. A complicating factor could be that the reference area of the airway in general, and of the airway at the EPP in particular, should be expected to increase with lung volume for airways receiving even indirect parenchymal support. Nevertheless, an EPP upstream from the trachea together with a substantial head loss to the EPP would appear to be the most plausible interpretation, one more in accord with the invasive and excised measurements.

Influence of gas density on the MEFV curve. Another

indication of the effect of friction in human lungs at moderate-to-high lung volumes is obtained from the comparison of the present predictions with the results of a hyperbaric study by Wood and Bryan (37). According to the predictions of the purely frictionless analysis, the critical rate of flow should be exactly proportional to the inverse square root of gas density for each value of static recoil pressure. But the experimental observation of this relationship of flow to density was significantly different, more like inverse proportionality to the 0.45 power, which is a value attributable to a detectable frictional effect. At lung volumes below 25% VC the inverse proportionality fell markedly, to about the 0.1 power, indicating a large frictional effect.

DISCUSSION

The functional basis of the sometimes close relationship between EPP and choke point is important to explore. Except for the case of a large frictional loss, the effect of the choke point is to set the maximum flow rate in the airway according to the local value of the head. The EPP, on the other hand, gives an indication of the location of substantial airway narrowing, which is the result of the choking that limits flow. The airway properties must be balanced so that the airways allow large enough values of flow ($AY^{1/2}$ large enough) while being small enough to develop high local velocities for an efficient cough (A small enough) and compliant enough to avoid excessive tissue stress (Y small enough). One result of this balance, which involves varying degrees of parenchymal support of airway walls at different airway locations and at different lung volumes, is the MEFV curve.

The MEFV curve for a power-law form of pressure-area function was shown in Fig. 5*C*. A somewhat similar curve, the dotted curve of Fig. 6*A*, was obtained for the same assumptions on the basic parameters, Aok = 2cmH_2O and Yok = 10cmH_2O, used with Fig. 4*D*, which is based on the Fry form of pressure-area function. More realistic assumptions for most lungs would take into account the dependence of the choke point properties upon lung volume, including the effect of location. An increase of elastic support of airways with increase of lung volume can be expected at locations that include the choke point, which seems likely from our above interpretation of experiments to stay near the location of the insertion bronchi into the parenchyma in some normal humans. The effect that such an increasing support with lung volume has on the MEFV curve was modeled by assuming that Yok increases linearly (from 5 to 30 cmH_2O) with Bv (from 0 to 20 cmH_2O) and that Aok = 2 cm^2. Then the solid MFSR curve of Fig. 6*A* was constructed from Fig. 4*D*, which represents the prediction on the basis of a Fry form of pressure-area function. The corresponding MEFV curve of Fig. 6*B* was constructed on the assumption of an averaged pressure-volume curve for humans aged 24–30 (27) (Fig. 6*C*).

An experimentally obtained MEFV curve for a human and one for a dog (22) are also shown in Fig. 6*B*. At lung volumes above the sharp bend at 25% VC, the dog curve follows the shape of the solid curve of the theoretical model. The human curve is steeper than either the dog or theoretical curve in that range of vital capacity,

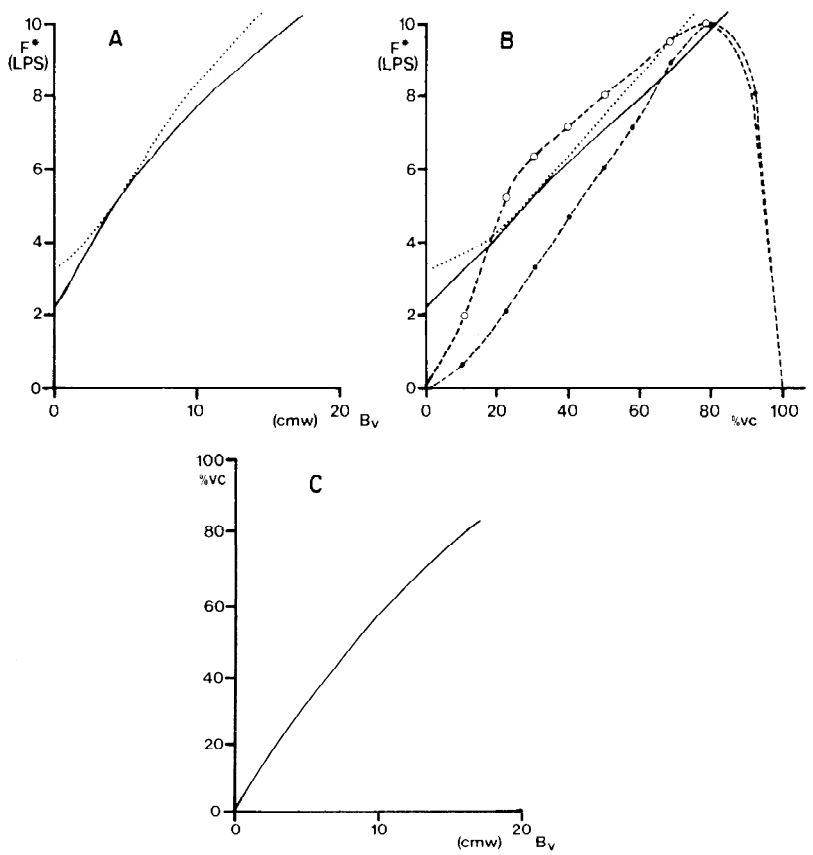

FIG. 6. *A*: MFSR curve constructed from Fig. 2*D*, Au/Ao = 2, Aok = 2 cm^2. (—) Yok increasing with lung volume, (····) Yok = 10 cmH_2O. *B*: MEFV curves: (—) (····) constructed from *A* and *C*, (- - - -) observed human curves, (– · –) observed dog curve (22). *C*: average pressure-volume curve for ages 24–30 (27). Horizontal scale was on the basis of a ratio RV/TLC equal to one-fifth.

as would be explained by effect of friction in humans, as discussed above, and to the reduction of Aok with lung volume due to the more peripheral human choke point losing support. At low lung volumes the theoretical predictions of flow rate are far too high. The change of shape of the dog curve below 25% VC is interpreted as indicating an abrupt peripheral movement of choke point, as well as substantial frictional effect. In humans the abrupt peripheral movement of choke point, indicated by density dependence above, is not evident in the MEFV curve. However, the observed low rates of flow near 0% VC, a few tenths of a liter per second, are not consistent with the lowest values of $AY^{1/2}$ that central airways with some cartilage support can achieve. Thus independently of the effect of friction, the inference is that the choke point must be quite peripheral and that the aggregate cross-sectional area of choke points in airways not effectively closed is of the order of 1 cm^2. Such peripheral locations of choke points at very low lung volumes would be consistent with the very peripheral location of EPP's observed in dogs at low lung volumes (14), with the suggestion that the effective closure of airways at low lung volumes is due to flow limitation (15, 34), and with the observation of histological closure at slightly negative recoil pressures (14).

In addition to these particular shapes of MEFV curves for man and dog, there are well known variants that may be explained by variations on the above reasoning. In humans these variants include curves that are less steep in some young normal adults and curves that become so steep as to become concave upward even at high lung volumes in older normal adults (27). In dogs there is a considerable variety of curves, some of which have no distinct bend (22), and induced bronchoconstriction can produce an MEFV curve that is entirely concave upward, as in Jones II.

Some of the experimental results interpreted in the previous section may be rather extreme versions of circumstances in the normal lung. One instance already cited is a possible bronchoconstriction which was induced by the catheter and which produced a peripheral shift of EPP. Another is that the process of opening the chest to expose the lung and, even more, the process of excision of the lung would be expected to reduce support for extraparenchymal airways, thus reducing Ao and Yo and increasing the likelihood that choke points would occur in these airways. This tendency for more central choke points would be reflected in a like tendency of EPP's, as observed (10). The observed reduction of flows and less steep MEFV curves at high lung volumes would also be consistent with increased friction resulting from reductions of cross-sectional area due to reduced airway support.

Conclusions

By appealing to the wave-speed concept of flow limitation, the present theory is able to offer a comprehensive explanatory framework for understanding flow limitation in forced expiration. This theory offers improved intuition to the work on mathematical modeling and an improved precision to the ideas of the intuitive models that have been used to explain the observations. Although the present work leans heavily on the wealth of knowledge of flow limitation of better known types in fluid mechanics, there may be some principles of critical flow in collapsible tubes that are of interest in general fluid mechanical theory as well.

One of the main clarifications offered for the intuitive models is that the "waterfall effect" (33) can be interpreted to be of the type of flow limitation that occurs at a constriction in an open channel. The present critical condition leads to a precisely defined choke point, critical area, and critical distending pressure, implying a precisely defined critical rate of flow, all of which are set by upstream conditions as well as the local airway properties at the choke point. Whether there is friction or not, the critical rate of flow is established for flow velocity reaching wave speed at the choke point, and a specific, widely applicable mechanism to maintain steady flow limitation is proposed: an elastic jump. The compressed segment of airway, as interpreted by the present theory, is seen as a functionally important result of the critical phenomenon of flow velocity being limited by wave speed. In principle, there need be no compression ($B < 0$) in the system at flow limitation. The condition that the choke point is not compressed ($B^* > 0$) is that the flow parameter F^*/Fok is greater than one; or equivalently the distending head at the choke point must be greater than $Yok/2$, as developed in APPENDIX C.

The present theory predicts the part of the geometry of the airways that is unchanged with increased effort for a fixed elastic recoil pressure. For any increase of effort above the critical value, the geometry upstream from the elastic jump does not change because, except for effects of longitudinal tension, the disturbance of the increase cannot propagate upstream through the region of flow having a velocity greater than wave speed. Because of the shape of the pressure-distance curves in Fig. 4*A* it is seen that there can be one EPP upstream from the jump and one downstream. Thus, according to the present theory, the argument of Mead et al. (27) of fixed geometry of stream of "the" EPP is necessarily valid only for that EPP which is upstream from the jump. Such an EPP is, therefore, within the fixed part of the geometry. The EPP is a useful experimental and theoretical benchmark, but in reasoning about mechanisms of critical flow the choke point has the great theoretical advantage of being intimately involved in the mechanism that is producing the limitation and at the same time must be physically very near a distinctive location, a local minimum of the static curve of area as a function of distance.

Apart from the problem of interpreting previous experiments by the present theory, as discussed above, one of the main difficulties in applying the present theory to any experiment is in locating the choke point and in ascertaining its properties, including dependence on lung volume. Even a well-defined minimum in the static area as a function of distance becomes an undistinguished point in the dynamic curve of pressure as a function of distance. There are also shortcomings of the scope of the present theory because of the need to con-

sider quantitatively the effect of friction, of longitudinal tension, and of asymmetry of the pathways. Overcoming such difficulties may produce a highly predictive theory, permitting better interpretation of existing forced expiratory tests and aiding in the design of improved tests.

SYMBOLS

The reason for our departure from some of the standard symbols of lung mechanics in this work is to attain clarity efficiently. Subscripts are indicated as lowercase letters on the line of their governing capital, as is now customary in lung mechanics. However, the customary descriptive subscript, as in Palv, is replaced by the single letter, as in Pv. In a double subscript the first subscript indicates the state, the second indicates the location. Thus Prp is the value of pleural pressure for the critical conditions. At an actual choke point, however, which is critical by definition, the pair of subscripts, r for critical state and k for location, is replaced by a star (*), as is a colorful convention in compressible flow theory. In the case of critical flow rate, F* is not only the indicated rate at the choke point, but also the actual flow rate for the entire tube system. The subscript o always indicates a reference state, which is the state B = 0, except when the o is a subscript on B itself. In that case it indicates one of the extreme states A = 0 or A = ∞.

Two capital symbol changes are made. *1*) The distending pressure function is assigned the symbol B for bronchial to avoid any additional use of qualifiers on P and to reserve P for pressure relative to customary references such as atmospheric pressure or the perfect vacuum. This assignment leads to the use of Bv for "static recoil pressure" of the lung. *2*) The instantaneous flow in the airway is assigned the symbol F, a return to an older notation. For incompressible expiratory flow, $F = -\dot{V}$ where $\dot{V}$ is the Newtonian symbolism for the rate of change of thoracic gas volume. In those cases in which gas compression is important, the present assignment permits a simple distinction to be made between the local flow rate and the rate of change of lung volume.

UNITS

The units quoted in the text are customary physiological units. However, the symbols for the physical variables are ultimately meant to imply quantities in a self-consistent system of units such as the proper cgs system, in which no gravitational factor appears. Thus, the governing form of units is obtained by converting liters ($1 = 10^3$ cm^3) and centimeters of water ($cmH_2O = 980$ dyn·cm^{-2}) to the proper cgs units. In some cases, for example in computing the flow parameter F/Fo, the customary physiological units (including $\rho = 1.14$ g/l BTPS) happen to give directly the correct dimensionless magnitude within 2 parts in 1,000.

APPENDIX A

Wave Speed

The concept, wave speed, is used in the main text to develop the mechanism of flow limitation as straightforwardly as possible. Only in a highly idealized dynamical model of an elastic tube would there literally be at each point the single wave speed referred to in the text. In such a (nondispersive) model, it is unnecessary to distinguish between the speed of traveling waves which propagate disturbances and the speed of the standing wave. In more realistic models of the tube's dynamic response, a fundamental wave-speed quantity, phase velocity (24), depends on frequency components in the wave, and such wave travel is termed dispersive. Dispersive waves occur in a tube model including such effects as the gas viscosity and compressibility and the wall inertance and viscance. Longitudinal tension in the tube wall produces a dispersive as well as a standing-wave effect, and the gas compressibility also produces a standing-wave effect. The dispersive effects are not of direct interest in the present work because it is ultimately only the standing wave that controls the flow limitation according to the present theory. The standing-wave effect of longitudinal tension was included in the distending pressure function of the main text. The standing-wave effect of gas compressibility is now treated.

The effect of gas compressibility upon the (standing) wave speed can be calculated by considering the gas compliance pathway in parallel with the wall compliance pathway. Thus $-\partial v/v\partial P$ is to be added to $\partial A/A\partial B$ to obtain the effective local specific compliance, the reciprocal of which is the local elastic modulus of the airway (tube). The resulting wave speed, which is the square root of the ratio of elastic modulus to (effective) fluid density is

$$\left\{q\rho\left(\frac{\partial A}{A\partial B}-\frac{\partial v}{v\partial P}\right)\right\}^{-1/2}=\left\{q\rho\left(\frac{1}{Y}+\frac{1}{\gamma P}\right)\right\}^{-1/2}$$

where v = local control volume, P = absolute pressure, and γ = ratio of specific heats. The value of this wave speed is seen to be less than both the wave speed in a tube with incompressible fluid and the wave speed in a tube with rigid walls. This latter wave speed is just that of sound, $(\gamma P/\rho)^{1/2}$, if the velocity profile is blunt (q = 1). Except in very large stiff airways Y is sufficiently smaller than γP that the wave speed closely approaches $(Y/q\rho)^{1/2}$, the value used in the main text; but it should be remembered that ρ is to be evaluated to take account gas compression generated by large pleural pressures.

APPENDIX B

Critical Condition, Frictionless Solutions, and the Jump

In this appendix, the methods of construction of Fig. 4 are presented. The first section is concerned with critical conditions of Fig. 4*D* and the subsequent sections treat the X dependence of Fig. 4*A*.

Critical condition. The condition for which flow is a maximum is instructively derived by considering the *local* value of distending head

$$J \equiv B + {}^1/_2 q\rho (F/A)^2 \qquad (B\text{-}1)$$

This is the head relative to pleural pressure: the sum of the distending pressure and the kinetic term. Figure 7*A* is here interpreted as a plot of J(A), from which it is apparent that a minimum of J(A) for fixed F is a maximum of F for fixed J. So the condition for maximum flow is $\partial J/\partial A = 0$, which implies in *Eq. B-1* that

$$(\partial B/\partial A) \quad q\rho F^2/A^3 = 0 \qquad (B\text{-}2)$$

which is just the wave-speed condition of *Eq. 5*. As outlined in the main text, the minimum along the airway of this maximum F defines the critical conditions of actual maximum flow.

For a choke point with an A dependence of B(A, X) as in Fig. 7*A*, the locus of minima shows that the critical rate of flow is strictly increasing, not only with A, but also with the local value of distending head. Identification of values of F/Fok along this locus gives Fig. 4*D*. A simple expression for this locus is obtained by substituting in *Eq. B-1* for F according to the condition of *Eq. B-2*. The result is *Eq. 4*.

Frictionless solutions. The continuous curves of Fig. 4*A* in the frictionless case are constructed by solving for B(A, X) in *Eq. 2*, where A is the inverse of the function B at each value of X. A plot of J/Yo for fixed values of F/Fo gives the solid curves of Fig. 7*A* in the dimensionless form

$$J/Yo = B/Yo + {}^1/_2(F/Fok)^2\,(Aok/Ao)^2\,(Ao/A)^2 \qquad (B\text{-}4)$$

where the definition of Fok was used. Now for the specified head ratio, J/Yo = 1, *Eq. B-4* is solved for A/Ao and therefore B/Yo at each location, Aok/Ao, and for each specified ratio of flow parameter, F/Fok. The frictionless curves, on the right of Aok/Ao = 1 in Fig. 7*A* are mirror images of the curves on the left.

The Jump. The condition on the jump from one solution curve to another in Fig. 4*A* is just that the net force on the jump is equal to the change of momentum rate through the jump (32). Thus in Fig. 8 the force, positive to the right, on the fluid in the control volume is

$$\begin{aligned} &P_1A_1 + \int_1^2 P(x)dA(X) - P_2A_2 + \text{shear} \\ &= (Pp + B_1)A_1 + \int_1^2 (Pp + B)dA - (Pp + B_2)A_2 + \text{shear} \\ &= B_1A_1 - B_2A_2 + \int_1^2 B\,d\Lambda + \text{shear} \qquad (B\text{-}5) \\ &= -\int_1^2 A\,dB + \text{shear} = I_2 - I_1 \end{aligned}$$

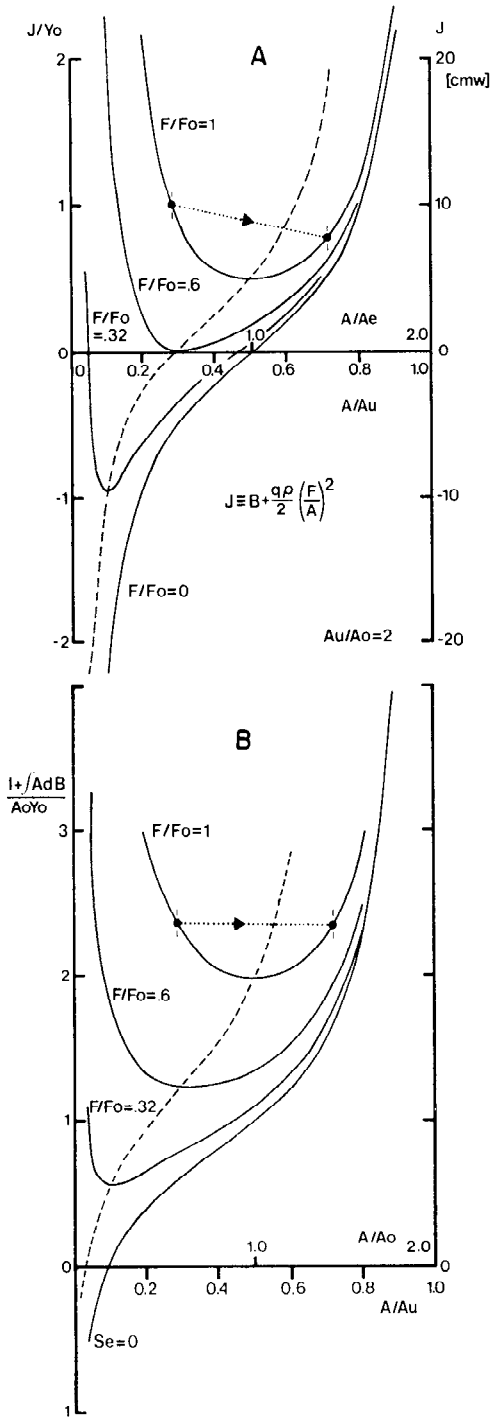

FIG. 7. *A*: distending head vs. area ratio for fixed speed parameter. *Dashed curve* is the locus of minima. *Dotted line* with negative slope connects two states at one of the elastic jumps in Fig. 2*A*. *B*: force-momentum-rate quantity conserved in the elastic jump, plotted against area ratio for fixed value of speed parameter F/Fo. *Dashed curve* is locus of minima. *Dotted horizontal line* connects the two states at one of the elastic jumps in Fig. 2*A*. Note that the larger areas and the smaller areas at the jump are the same in *B* and *A*.

where I = $q\rho U^2A = q\rho F^2/A$ = momentum rate. Because the shear from the wall friction is expected to be relatively negligible, the quantity which is approximately conserved across the jump is

$$q\rho F^2/A + \int A\, dB$$

where the lower limit of integration is fixed at a convenient value.

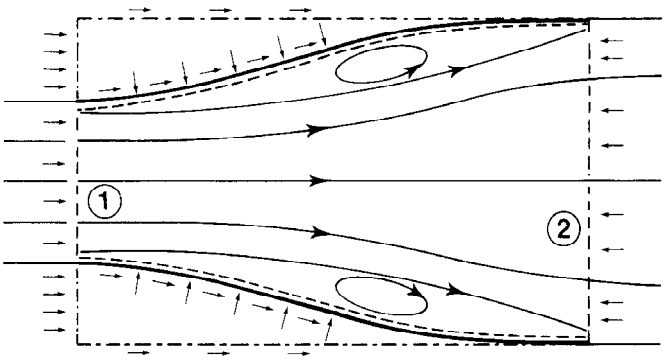

FIG. 8. Schematic diagram of force balance for an elastic jump. *Solid curves* represent streamlines of the idealized flow. Note *closed curves* representing standing eddies. *Dashed curve* (– –) encloses the control volume for the force balance on the fluid between the smaller cross section (*1*) at super critical velocity on *left* and the larger cross section (*2*) at subcritical velocity on *right*. Inner surface of the tube between two sections forms the intervening surface of control volume. Small detached arrows represent distributed forces on the surfaces shown, pressures being perpendicular to the surface and shear forces being tangential to the surface. *Dash-dot* (–·) *lines* are shown for convenience in calculating horizontal component of actual forces on the curved surface of the tube.

This result is just that of Oates (28) but not that of Lambert (19).[4]

As a particular example of this force-balance quantity, the Fry form for area dependence, *Eq. 7*, gives the following U-shaped function, plotted in Fig. 7*B*

$$\frac{q\rho F^2}{YoAo^2}\frac{Ae}{A} + \frac{Au-Ao}{Au}\int \frac{A}{Ao}\, d\left[-\frac{Ao}{A} + \frac{Au-Ao}{Au-A}\right] = \left(\frac{F}{Fo}\right)^2 \frac{Ao}{A} \qquad (B\text{-}6)$$

$$+ \frac{Au-Ao}{Au}\left\{\mathrm{Ln}\left(\frac{A}{Ao}\right) + \frac{Au-Ao}{Ao}\left[\mathrm{Ln}\left(\frac{Au-A}{Ao}\right) + \frac{Au}{Au-A}\right]\right\}$$

For each value of F/Fo and Au/Ao and for each value of this force-balance quantity down to the minimum value, the two values of A/Ao across a jump are determined. The direction of the jump is from lower to higher value of area, corresponding to a jump in velocity from greater than to less than wave speed. This choice ensures that head is lost rather than gained across the jump, as is seen in Fig. 7, by comparing, for a given F/Fo, the values of head corresponding to the smaller and the larger values of A/Ao that are determined by a single value of the force-balance quantity. At the minimum value of the force-balance quantity the critical condition is attained and the two values of area are equal; so the jump becomes of zero height as it approaches the choke point.

The jumps in Fig. 4*A* were calculated as follows. *1*) The critical flow conditions establish the portion of the frictionless solution curve that has a velocity greater than wave speed (CD in Fig. 4*A*). Thus for given J/Yok, F*/Fok is established, and according to *Eq. 2* the area ratio A(X)/Ao(X) is established as a function of the location variable, Ao(X)/Aok

$$\frac{J}{Yok} = \frac{B}{Yok} + \frac{q\rho}{2}\left(\frac{F^*}{AokYok^{1/2}}\frac{Aok}{Ao}\frac{Ao}{A}\right)^2 \qquad (B\text{-}7)$$

2) According to the definitions involved

$$\frac{F^*}{Fok} = \frac{F^*}{Fo}\frac{Fo}{Fok} = \frac{F^*}{Fo}\frac{AoYo^{1/2}}{AokYok^{1/2}} = \frac{F^*}{Fo}\frac{Ao}{Aok} \qquad (B\text{-}8)$$

where the constancy, Yo = Yok, was used to get the last expression on the right. Hence, a choice of F*/Fo fixes the location. So according to *Eq. B-7* the area ratio A/Ao is fixed. *3*) This value of A/Ao fixes the value of the force-balance quantity on the descending limb (smaller

[4] J. W. Lambert's statement of elastic jump conditions is just that of a hydraulic jump; so it does not include a variation of hydrostatic pressure on the face of the jump (19), which variation is included in the present elastic jump conditions (28).

area) of the curve with the chosen value of F/Fo in Fig. 7*B*. So the value of A/Ao on the ascending limb of the same curve is fixed in turn. *4*) The reduced value of head ratio for the larger area ratio at the jump is calculated from *Eq. B-7* or constructed from Fig. 7. With this value of head the area ratio for the frictionless flow downstream from the jump is directly calculated from *Eq. B-7*.

APPENDIX C

Choke Point Properties and the Power-Law Form of Area Dependence

Key mathematical properties of solutions in the vicinity of the choke point are developed. The correspondence between the area dependence of distending pressure at the choke point and the flow as a function of head at the choke point is demonstrated generally. Then relationships for the power-law form of area dependence are derived and used to illustrate the correspondence of Ak(Bk) and F*(J*). Other relationships such as that of head and pressure at the choke point and that of choke point and EPP are derived.

Choke point properties from critical flow versus head. In the main theory section on critical conditions and again at the beginning of APPENDIX B it was shown essentially that if the area dependence of B(A, X) is specified at the choke point, then so also is the relationship between the head there and the critical flow rate. In particular if friction in airways is negligible, then B(A, Xk) implies a specific MFSR relationship. The converse is also true: if maximum flow and head at the choke point are specified, then so also is B(Ar, Xk). The explicit demonstration of this principle leads to formulas that may be of interest in applications.

First the distending head at the choke point is defined as in *Eq. B-1*

$$J^* = B^* + {}^1/_2 q\rho (F^*/A^*)^2 \qquad (C\text{-}1)$$

Now F* can be considered simply a function of A*. So by the chain rule for differentiation

$$\frac{dJ^*}{dF^*} = \left(\frac{\partial B}{\partial A} - q\rho \frac{F^2}{A^3}\right)^* \frac{dA^*}{dF^*} + q\rho \frac{F^*}{(A^*)^2}$$

But the quantity in round brackets vanishes by virtue of the critical condition of *Eq. 6*. So the remainder of the equation is solved to get A* purely in terms of F* and J*

$$(A^*)^2 = q\rho F^* (dF^*/dJ^*) \qquad (C\text{-}2)$$

Then A* is eliminated between this relation and *Eq. C-1* to give

$$B^* = J^* - {}^1/_2 F^* (dJ^*/dF^*) \qquad (C\text{-}3)$$

Equations C-2 and *C-3* together provide an explicit representation of B*(A*) from sufficient measurements of J* and F*. In using these equations in practice, it is important to keep account of head loss in estimating J* from the value of head, for example Bv, at a remote location. It is also important to note that in typical cases in which the area dependence of B(A, Xk) depends on lung volume (13), the function B*(A*) is a locus of points each of which may be on a different curve of pressure versus area. In that case Y* is not obtained from dB */dA* but directly from *Eq. 6*.

Power-law form of area dependence. In further developing the mathematics of critical relationships, it is convenient to adopt a power-law form of pressure-area function at the choke point. In contrast to certain blood vessels, the central airways are not expected to satisfy any one power-law form over a wide range of pressures; so several different power-law forms will generally be required to cover a wide range of pressure. The power-law expression for B(A, Xk) can be developed by considering that the elastic modulus at the choke point is of the form

$$Y = A\, dB/dA = Z_1 A^n \qquad (C\text{-}4)$$

where Z_1 = constant of proportionality and n = a constant real power. Dividing this equation by A and integrating gives

$$B(A, X) \equiv B = n^{-1} Z_1 A^n + Bo \qquad (C\text{-}5)$$

where Bo is the constant of integration.

The constants Z_1 and Bo are readily interpreted in *Eq. C-5*. To ensure that A be real for all admissible n it is necessary that B $\gtrless$ Bo according as ($\Leftrightarrow$) n $\gtrless$ 0. See also the form of *Eq. 8*. For n > 0 Bo is the value of B at A = 0 and for n < 0 Bo is the value of B at A = ∞. The scaling or proportionality constant, Z_1, is then simply equal to Y/A^n for all A (S. Permutt, communicated in review). If the B(A) relation to be described by a power law has a (real, positive) intersection with the A axis the reference state as defined in connection with *Eq. 7* can be used to replace the parameterization in Z_1 and Bo by one in Ao and Yo, using *Eqs. C-4* and *C-5*

$$Z_1 = Yo/Ao^n = Z^{-n} \qquad (C\text{-}6)$$

$$Bo = -n^{-1} Z_1 Ao^n = -Yo/n \qquad (C\text{-}7)$$

Thus, in this important special case *Eq. C-5* can be written in a form analogous to *Eq. 7*

$$B/Yo = n^{-1}[(A/Ao)^n - 1] \qquad (C\text{-}8)$$

There is also an obvious further restriction necessary to ensure the intersection of B(A) with the A axis

$$Bo \gtrless 0 \Leftrightarrow n \lesseqgtr 0$$

The parameterization of the power law based on Ao and Yo is developed in the present work because the reference state, B = 0, is expected to be near the actual critical value of distending pressure in the airways and this parameterization also allows a convenient comparison to the Fry form of *Eq. 7*. In cases of no intercept of B(A) on the A axis, the parameterization based on Z_1 and Bo is valid while that based on Ao and Yo is not. The use of Z_1 and Bo is also very convenient for circumstances such as a pure shift of the B(A) curve, as occurs for a bronchoconstriction that has the effect of requiring the same increase of distending pressure to return to a cross section to its original area, no matter what the value of that area.

Correspondence for the power-law case. A demonstration of how the relationship between the head J* at the choke point and the critical flow rate F* corresponds to B(A, Xk) is outlined in the power-law case. This correspondence could be developed from *Eq. C-5* as in the construction of Fig. 2, but it is instructive here to use the earlier equations of this appendix to go in the opposite direction – from F*(J*) to the choke point area dependence. Let critical flow rate be assumed as the power-law function of recoil pressure of *Eq. 9*, where W and m are to be determined. Then F* and dF*/dJ* are readily evaluated in *Eqs. C-2* and *C-3* to obtain

$$A^* = (q\rho)^{1/2} W[m(J^* - Bok)]^{1/n} \qquad (C\text{-}9)$$

$$B^* = J^* - \frac{m}{2}(J^* - Bok) \qquad (C\text{-}10)$$

Now *Eq. C-9* is readily solved for J*, which may then be eliminated from *Eq. C-10* to obtain *Eq. 8* in the main text if the relations of *Eqs. 10a* and *10b* are used. The correspondence is illustrated in Fig. 9. From the simple form of *Eqs. 8* and *9* a pure shift of A(B) to the right, which is an increase of Bo at fixed Z, is seen to be matched by an identical shift of F(J*) to the right. An increase in Z_1 (elastic modulus for n = 0) at fixed Bo results in a *decrease* or increase in W, and therefore F*, according to whether n is *greater* or less than zero.

An instructive example of the power-law form of pressure-area function is that of n = 2, corresponding to m = 1, implying a linear relationship between head at the choke point and maximum flow rate, *Eq. 9*. For the frictionless case, this relationship has a strong resemblance to the Eq. 2 of Pride et al. (33), where W^{-1} would be called a "resistance." The difference is that our Bok in *Eq. C-9* is replaced by their critical transmural pressure Ptm', which in that work is in the spirit of our B*, whereas the Ptm' of their earlier work was defined essentially as our Bok (S. Permutt, communicated in review).

Another application of this prediction is in pursuing the reasoning of Mead et al. about the shape of the MFSR curve (25). The present prediction is that for a fixed choke point with constant properties and for frictionless flow there is a variety of possible MFSR curves, for example those with shapes made up of cases, n = 1, n = 2 and n = ∞ in Fig. 8*B*. The case, n = ∞, which corresponds to the assumption of a fixed EPP in Fig. 5A of Mead et al. is the limiting case of an infinitely stiff tube. Their less steep curves for an increasing area of EPP are physically impossible in the context of the above assump-

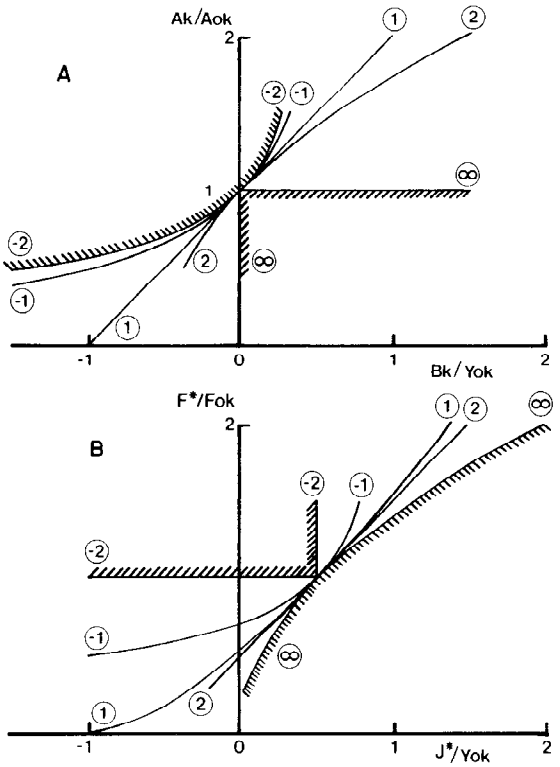

FIG. 9. Power-law forms. *A*: area dependence of distending pressure functions. *B*: MFSR curves. *Circled numbers* give the power n. *Cross-hatching* represents bounds on the physically possible regions. Note that all the curves represent increasing functions.

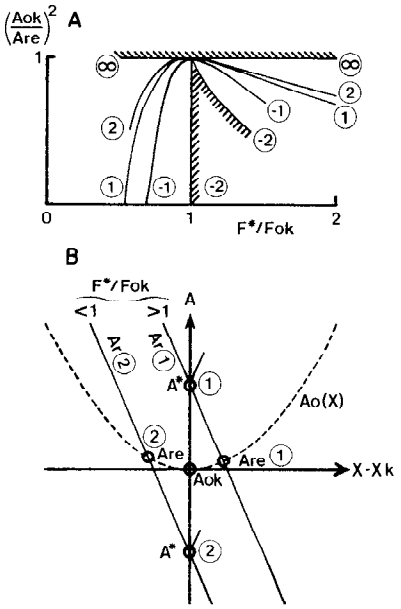

FIG. 10. Relationship of EPP and choke point. *A*: power-law result for ratio of reference area at the choke point to reference area at the EPP. *B*: schematic representation of predictions *in the neighborhood* of the choke point. Reference-area Ao(X) curve is a (*dashed*) parabola; so the critical solutions Ar(X) are (*solid*) straight lines, bifurcating at the choke point (X = Xk) into a critical branch of increasing area (S < 1) and a branch with supercritical velocity and decreasing area. *Curve 1* attains an EPP downstream from the choke point only, on the branch with supercritical velocity. *Curve 2* has an EPP upstream from the choke point and may also have on downstream.

tions. However, if the choke point properties change appropriately, so that the reference area of the choke point increases sufficiently with decreasing lung volume, then a less steep MFSR would be obtained. Much steeper MFSR curves than those implied by the above assumptions are predicted for effects associated with decreasing lung volume. One is the effect of friction and the other is the effect of decreasing stiffness for F*/Fok less than unity as explained in connection with Fig. 4*D*.

Head and pressure at choke point. Though not readily measurable directly,[5] the relationship between B* and J* is one that is likely to be of interest in experiments, particularly in the case of negligible friction, implying that J* approximates Bv. Subtracting Bok from both sides of *Eq. C-10* gives

$$B^* \quad Bok = \frac{2}{2 + n}(J^* \quad Bok) \qquad (C\text{-}11)$$

In this linear relationship the slope is always positive because $n > -2$.

EPP related to choke point. The EPP is defined as the location at which B = 0; so *Eq. 2* implies that

$$J^* = {}^1/_2 q\rho (F/Ae)^2 \qquad (C\text{-}12)$$

where e is the subscript for location of EPP. This equation can be used to obtain the ratio of reference area at the choke point to that at the EPP as a function of the flow parameter F*/Fok. In the case of a power-law form for area dependence of distending pressure, it is only necessary to use *Eq. 9* to evaluate J*, leading to

$$\left(\frac{Aok}{Ae}\right)^2 = 2\left(\frac{Fok}{F^*}\right)^2\left(\frac{1}{m}\left(\frac{F^*}{Fok}\right)^m - \frac{1}{n}\right) \qquad (C\text{-}13)$$

This relationship is plotted in Fig. 10*A*. It is seen that the reference area at the choke point is always less than the area at the EPP.

The actual variation of area in the vicinity of the choke point can be computed from *Eq. 2* for F − F*. A schematic plot is shown in Fig. 10*B* for the power-law case. In the applications a particularly important aspect of this plot is the relationship of A* to Ae, which indicates whether the choke point is upstream or downstream from the EPP for the solution curve 1CD in Fig. 4*A*. For any specific area dependence, and assuming there is negligible friction between choke point and EPP

$$J = B^* + {}^1/_2 Y^* = {}^1/_2 q\rho (F/Ae)^2 = {}^1/_2 Y^*(A^*/Ae)^2$$

or

$$B^* = {}^1/_2[(A^*/Ae)^2 - 1]Y^*$$

But since $Y^* > 0$

$$A^*/Ae \gtrless 1 \Leftrightarrow B^* \gtrless 0$$

which is the desired relationship. Also, because of the critical relationship

$$\frac{F^*}{Fok} = \frac{(AY^{1/2})^*}{Aok\,Yok^{1/2}}$$

and because $(AY^{1/2})^*$ is an increasing function of A*, it follows that

$$F^*/Fok \gtrless 1 \Leftrightarrow A^*/Aok \gtrless 1$$

with equality for Ae = Aok. Furthermore, directly from *Eq. 4*, if J* is

[5] From the definition, B* = P* − Prp; so if B* is inferred from airway properties and P* is approximated by consideration of head loss from choke point to mouth, then Prp can also be predicted to compare with measurements. Measurements show Prp to increase with lung volume, at least at the higher lung volumes (J. Mead, personal communication), while the present predictions of B* also increase with lung volume. The resulting implication that P* increases with lung volume at higher lung volumes is consistent with the observed increase of critical flow rate with lung volume, at least if a large share of P* is due to head loss in the upper airway with its fixed Rohrer constants.

an increasing function of A*, as must be the case for $AkYk^{1/2}$ increasing with Ak, then

$$J^*/Yok \geq 1/2 \Leftrightarrow A^*/Aok \geq 1$$

We gratefully acknowledge the substantial contributions of J. Mead to this work, including his guidance by searching review of our manuscripts. We have attempted to cite in the text the points at which some of his suggestions were used, but one suggestion not cited was his idea expressed to one of us years ago that flow limitation must have some clear physical basis such as the speed of sound, a basis similar to what we have developed. We are grateful for informal sessions and/or correspondence with many of the workers who have made major contributions in "flow-volume" research. We were particularly fortunate in having a stimulating and extensive journal review of the manuscript by S. Permutt. We are grateful for advice and encouragement from the bioengineers A. Shapiro, T. McMahon, and M. Y. Jaffrin, who had already been considering flow limitation in elastic tubes. We gratefully acknowledge informative discussion with our close colleague, James P. Butler.

This research was supported by Program Project Grant HL-14580 of the National Heart and Lung Institute.

Received for publication 21 April 1976.

REFERENCES

1. Chow, V. T. *Open-Channel Hydraulics*. New York: McGraw, 1959, p. 217–248, 393–438.
2. Clément, J., K. P. van de Woestijne, and J. Pardaens. A general theory of respiratory mechanics applied to forced expiration. *Respiration Physiol.* 19: 60–79, 1973.
3. Culver, B., J. Friend, V. Loverde, and J. Butler. The flow limiting segment in the airway (Abstract). *Physiologist* 16: 293, 1973.
4. DeGraff, A. C., Jr., and A. Bouhuys. Mechanics of air flow in airway obstruction. *Ann. Rev. Med.* 24: 111–134, 1973.
5. Elliott, E. A. *A Model of Maximal Expiratory Flow in Lungs* (MS thesis). Cambridge, Mass.: Massachusetts Institute of Technology, 1974.
6. Elliott, E. A., and S. V. Dawson. Test of wave-speed theory of flow limitation in elastic tubes. *J. Appl. Physiol.: Respirat. Environ. Exercise Physiol.* 43: 516–522, 1977.
7. Fry, D. L. Theoretical considerations of the bronchial pressure-flow-volume relationships with particular reference to the maximum expiratory flow volume curve. *Phys. Med. Biol.* 3: 174–194, 1958.
8. Fry, D. L. A preliminary model for stimulating the aerodynamics of the bronchial tree. *Computers Biomed. Res.* 2: 111–134, 1968.
9. Fry, D. L., and R. E. Hyatt. Pulmonary mechanics: a unified analysis of the relationship between pressure, volume, and gas flow in the lungs of normal and diseased human subjects. *Am. J. Med.* 29: 672–689, 1960.
10. Gardiner, A. J., L. Wood, P. Gayrard, H. Menkes, and P. Macklem. Influence of constriction in central or peripheral airways on maximal expiratory flow rates in dogs. *J. Appl. Physiol.* 36: 554–560, 1974.
11. Griffiths, D. J. Hydrodynamics of male micturition. I & II. *Med. Biol. Eng.* 9: 581–596, 1971.
12. Griffiths, D. J. Negative resistance effects in flow through collapsible tubes. *Med. Biol. Eng.* 13: 785–802, 1975.
13. Hughes, J. M. B., H. A. Jones, A. G. Wilson, B. J. B. Grant, and N. B. Pride. Stability of intrapulmonary bronchial dimensions during expiratory flow in excised lungs. *J. Appl. Physiol.* 37: 684–694, 1974.
14. Hughes, J. M. B., D. Y. Rosenzweig, and P. B. Kivitz. Site of airway closure in excised dog lungs: histologic demonstration. *J. Appl. Physiol.* 29: 340–344, 1970.
15. Hyatt, R. E., G. C. Okeson, and J. R. Rodarte. Influence of expiratory flow limitation on the pattern of lung emptying in normal man. *J. Appl. Physiol.* 35: 411–419, 1973.
16. Jones, J. G., R. B. Fraser, and J. A. Nadel. Prediction of maximum expiratory flow rate from area-transmural pressure curve of compressed airway. *J. Appl. Physiol.* 38: 1002–1011, 1975.
17. Jones, J. G., R. B. Fraser, and J. A. Nadel. Effect of changing airway mechanics on maximum expiratory flow. *J. Appl. Physiol.* 38: 1012–1021, 1975.
18. Jones, R. T. Blood flow. *Ann. Rev. Fluid Mech.* I: 223–244, 1969.
19. Lambert, J. W. On the nonlinearities of fluid flow in nonrigid tubes. *J. Franklin Inst.* 266: 83–102, 1958.
20. Lambert, R. K., and T. A. Wilson. A model for the elastic properties of the lung and their effect on expiratory flow. *J. Appl. Physiol.* 34: 34–48, 1973.
21. Macklem, P. T., and J. Mead. Factors determining maximum expiratory flow in dogs. *J. Appl. Physiol.* 25: 159–169, 1968.
22. Macklem, P. T., and N. J. Wilson. Measurement of intrabronchial pressure in man. *J. Appl. Physiol.* 20: 653–663, 1965.
23. Martin, H. B., and D. F. Proctor. Pressure-volume measurements on dog bronchi. *J. Appl. Physiol.* 13: 337–343, 1958.
24. McDonald, D. A. *Blood Flow in Arteries* (2nd ed.). Baltimore, Md.: Williams & Wilkins, 1974, p. 283–308.
25. Mead, J. Respiration: pulmonary mechanics. *Ann. Rev. Physiol.* 35: 169–192, 1973.
26. Mead, J., T. Taskishima, and D. Leith. Stress distribution in lungs: a model of pulmonary elasticity. *J. Appl. Physiol.* 28: 596–608, 1972.
27. Mead, J., J. M. Turner, P. T. Macklem, and J. B. Little. Significance of the relationship between lung recoil and maximum expiratory flow. *J. Appl. Physiol.* 22: 95–108, 1967.
28. Oates, G. C. Fluid flow in soft-walled tubes. *Med. Biol. Eng.* 13: 773–784, 1975.
29. Olsen, J. H., and A. H. Shapiro. Large-amplitude unsteady flow in liquid-filled elastic tubes. *J. Fluid Mech.* 29: 513–538, 1967.
30. Pardaens, J., K. P. van de Woestijne, and J. Clément. A physical model of expiration. *J. Appl. Physiol.* 33: 479–490, 1972.
31. Pederson, O. F. *The Mechanics of the Expiration Evaluated by a Model* (thesis). Aarhus, Denmark: Marselisborg Hospital, Institute of Physiology, 1973.
32. Prandtl, L. *Essentials of Fluid Dynamics*. New York: Hafner, 1953, p. 86–97, 161–168, 259–281.
33. Pride, N. B., S. Permutt, R. L. Riley, and B. Bromberger-Barnea. Determinants of maximal expiratory flow from the lungs. *J. Appl. Physiol.* 23: 646–662, 1967.
34. Rehder, K., A. R. Frazier, A. D. Sessler, J. R. Rodarte, and R. E. Hyatt. Closing volume for individual lungs (Abstract). *Federation Proc.* 34: 403, 1975.
35. Takishima, T., H. Sasaki, and T. Sasaki. Influence of lung parenchyma on collapsibility of dog bronchi. *J. Appl. Physiol.* 38: 875–881, 1975.
36. Weibel, E. R. *Morphometry of the Human Lung*. Berlin: Springer-Verlag, 1963, p. 123–125, 136–140.
37. Wood, L. D. H., and A. C. Bryan. Effect of increased ambient pressure on flow-volume curve of the lung. *J. Appl. Physiol.* 27: 4–8, 1969.